OXFORD UNIVERSITY PRESS | Carcinogenesis

SNAIL regulates gastric carcinogenesis through CCN3 and NEFL

Journal:	*Carcinogenesis*
Manuscript ID	CARCIN-2020-00184.R1
Manuscript Type:	Original Article
Date Submitted by the Author:	12-Nov-2020
Complete List of Authors:	CHEN, RU; Kyoto Daigaku, Graduate school of medicine Takaishi, Shigeo; Kyoto Daigaku, Graduate School of Medicine Masuo, Kenji; Kyoto Daigaku, Graduate school of medicine Yokoyama, Shoko; Kyoto Daigaku, Graduate school of medicine yogo, akitada; Kyoto Daigaku, Graduate School of Medicine Sugiyama, Aiko; Kyoto Daigaku, Graduate school of medicine Seno, Hiroshi; Kyoto Daigaku, Department of Gastroenterology and Hepatology Yoshizawa, Akihiko; Kyoto Daigaku, Department of Diagnostic Pathology
Keywords:	Gastric Cancer, Cancer Stem Cells, EMT, spheroid

SNAIL regulates gastric carcinogenesis through CCN3 and NEFL

Role of SNAIL/CCN3/NEFL axis in gastric cancer

Ru Chen[1,2], Kenji Masuo[1,2], Akitada Yogo[1,3], Shoko Yokoyama[1], Aiko Sugiyama[1], Hiroshi Seno[1,2], Akihiko Yoshizawa[4], Shigeo Takaishi[1,*]

1: DSK Project, Medical Innovation Center, Graduate School of Medicine, Kyoto University, Kyoto, Japan.

2: Department of Gastroenterology and Hepatology, Graduate School of Medicine, Kyoto University, Kyoto, Japan.

3: Department of Hepato-Biliary-Pancreatic Surgery and Transplantation, Graduate School of Medicine, Kyoto University, Kyoto, Japan.

4: Department of Diagnostic Pathology, Kyoto University Hospital, Kyoto, Japan.

*Corresponding author: Shigeo Takaishi; takaishi.shigeo.7w@kyoto-u.ac.jp

Abstract

Among cancer cells, there are specific cell populations of whose activities are comparable to those of stem cells in normal tissues, and for whom the levels of cell dedifferentiation are reported to correlate with poor prognosis. Information concerning the mechanisms that modulate the stemness like traits of cancer cells is limited. Therefore, we examined five gastric cancer cell lines and isolated gastric oncospheres from three gastric cancer cell lines. The gastric cancer cells that expanded in the spheres expressed relatively elevated proportion of CD44, which is a marker of gastric cancer stem cells, and displayed many properties of cancer stem cells, for example: chemoresistance, tumorigenecity and epithelial-mesenchymal transition (EMT) acquisition. SNAIL, which is a key factor in EMT, was highly expressed in the gastric spheres. Microarray analysis in gastric cancer cell line HGC27 showed that CCN3 and NEFL displayed the greatest differential expression by knocking down of SNAIL; the former was up-regulated and the latter down-regulated, respectively. Down-regulation of CCN3 and up-regulation of NEFL gene expression impaired the SNAIL-dependent EMT activity: high tumorigenicity, and chemoresistance in gastric cancer cells. Thus, approach that disrupts SNAIL/CCN3/NEFL axis may be credible in inhibiting gastric cancer development.

Keywords: Gastric Cancer; Cancer Stem Cells; EMT; spheroid

Introduction

Gastric cancer is one of the most common cancers in East Asia and Eastern Europe [1]. It is important to critically assess the current advances in our understanding of gastric cancer and to establish novel and innovative therapeutic strategies. A vast body of literature has been published on specific aspects of cancer initiating cells and on putative cancer stem cells (CSCs) which possess properties of stem cells distinct from differentiated progeny cancer cells [2]. Discovering significant genes and signaling pathways involving gastric cancer stemness could be helpful approaches to discovering novel therapeutic options.

During malignancy transformation, a critical process named the epithelial-mesenchymal transition (EMT) commonly occurs, and cells usually undergo a rapid change from differentiated and polarized epithelial state into an invasive mesenchymal composition [3]. During the development of diverse solid tumors, stem cell like traits were reported to be related to EMT. For example, after breast cancer cells acquired stem cell like features, the passaged mammosphere cells manifest with similar features to breast cancer stem cells, indicating a fundamental link between malignancy propagation and stem cell characteristics [4-6]. Among all the major EMT transcription factors, SNAIL, a zinc-finger protein, whose activities in relation to the downregulation of E-cadherin in colon cancer have previously been reported [7, 8]; binds to the E-boxes in the *CDH1* gene promoter and represses transcription of the *CDH1* gene [9]. So far SNAIL has been reported to contribute in many malignancy progression, and its' function in gastric cancer needs to be uncovered further as well. The precise mechanism of SNAIL-induced cell dedifferentiation and how this gene

can provide stem cell like traits in gastric cancer cells remain open to debate and to be further clarified. The discovery of genes under SNAIL regulation that could also be an instrumental breakthrough and lead to the establishment of novel therapeutic strategies in EMT-related stemness and malignancy. In the present study, we extracted CCN3 and NEFL as targets in the downstream of SNAIL, and determined the association of these two factors with stem cell like activity in gastric cancer cells.

Materials and Methods:

Cell culture, tissue collection and sphere growth

Human gastric cancer cell lines were purchased from RIKEN (https://cell.brc.riken.jp/ja/quality/str), JCRB cell bank (https://cellbank.nibiohn.go.jp/about-qc_english/), and ATCC (https://www.atcc.org/Services/Testing_Services/Cell_Authentication_Testing_Service.aspx), in which STR analysis is performed in these cell line banks to ensure the authentication of human cell lines, and were cultured according to the instructions provided by the manufacturer. Cell lines including human gastric cancer cell lines (HGC27, NCI-N87, GSU, MKN74, MKN45, NUGC3 and IM95), and embryonic kidney 293T cells were cultured in DMEM (Nacalai Tesque, Japan) supplemented with 10% fetal bovine serum (HyClone Defined Fetal Bovine Serum (FBS), USA) and penicillin-streptomycin mixed solution (10,000u/ml, Nacalai Tesque, Japan). For RNA extraction from each cell line, NucleoSpin RNA Plus (Takarabio, Japan) was used following the manufacturer's instructions. The preparation of paraffin-embedded blocks was performed as follows: slices of tumor formed from each of the cell lines were immersed in 4% paraformaldehyde (Nacalai Tesque, Japan) to allow the assembling of paraffin-embedded blocks. Cells were cultured in homemade stem cell medium (DMEM/F12 supplemented with B27 Supplement (ThermoFisher), 10 ng/mL recombinant basic fibroblast growth factor (bFGF, ThermoFisher), 10 ng/mL epidermal growth factor (EGF, ThermoFisher), and 1% penicillin-streptomycin) to obtain spheres. A total of 1 x 10^4 cells per milliliter were seeded in culture medium for stem cell

and incubated in ultra-low attachment plates for 5 days. Spheres larger than 80 μm in diameter were counted using Cell3Imager (InSphero AG and Dainippon SCRREEN, Kyoto, Japan). TrypLE Express (ThermoFisher) or Trypsin-EDTA (FUJIFILM Wako, Japan) were used to separate cells from the floating spheres and adherent cells to allow cell counting and other experiments.

In vivo tumorigenicity assay

All procedures involving animals were conducted in accordance with the Institutional Animal Welfare Guidelines of Kyoto University. NOD/SCID mice were purchased from the Charles River Laboratories (Yokohama, Japan) and were maintained according to the Guidelines for Laboratory Animals in the Kyoto University. The tumorigenicity assay was performed by subcutaneous injection of 1 x 10^4 designated cells into the flanks of 8- to 10-week-old NOD/SCID mice. Mice were sacrificed and examined for tumor harvest once the tumor had reached pre-determined size (2.5cm maximum). Tumor size was measured with calipers once a week after the injection.

Lentivirus production, short-hairpin RNA-mediated human SNAIL gene knockdown and stable clone establishment

The lentivirus package system: pMDLg/pRRE (Addgene, plasmid #12251), pRSV-Rev (Addgene, plasmid #12253) and pMD2.G (Addgene, plasmid #12259) together with the shRNA plasmid targeting the human SNAIL gene as well as the control vector: pLKO.1puro (Addgene, plasmid #8453) were co-transfected into 293T cells by Lipofectamine 3000 (Invitrogen). SNAIL-targeting short-hairpin RNA (MISSION shRNA)

duplex (A: 5-TGCTCCACAAGCACCAAGAGTC-3; B: 5-CCACTCAGATGTCAAGAAGTAC-3) and NEFL-targeting short-hairpin RNA (MISSION shRNA) (5-CGACAGCTTGATGGACGAAAT-3) were purchased from Sigma-Aldrich Co. LCC. (St. Louis, MO, USA). About 48 to 72 hours later, virus supernatant was collected for concentration. For shRNA knockdown, HGC27 and IM95 cells were seeded onto 6-well plates and infected with optimal virus concentrations supplemented with 6 μg/mL Polybrene (Sigma, St. Louis, MO, USA), then incubated for 12 hours before replacing with fresh medium. Cells were then selected by puromycin (INVIVOGEN, Japan) at the concentration of 1.8 μg/ml (HGC27) and 4 μg/ml (IM95) for 2 weeks.

Transient transfection

Lipofectamine 3000 reagent was used for the introduction of overexpression vectors to establish stable lines, including the NEFL (Sino Biol.HG13214-UT), CCN3 (Sino Biol.HG10264-UT) and SNAIL (Sino Biol.HG16844-UT) overexpression vectors and matched control vector (Sino Biol.CV011), all of which were purchased from Sino Biological Inc. (Wayne, PA, USA). Selections were carried out via hygromycin B (Nacalai Tesque, Japan); resistance and transfection efficiency were verified through real-time qPCR.

Microarray data and bioinformatics analysis

Total RNA from each sample was extracted using NucleoSpin RNA Plus kit, forwarded with Affymetrix Human Genome U133 Plus 2.0 Array (HuGene2.9st, Japan) analysis. RNA extraction, microarray hybridization, and feature selection were performed

according to the manufacturer's protocol. Microarray data can be download from the GEO database (https://www.ncbi.nlm.nih.gov/geo/query/acc.cgi?acc=GSE145867). Bioinformatics and genetic network construction were performed in R Studio (version 1.2.1335) mainly using RMA [10] from the affy package [11] and the GoPlot package (https://CRAN.R-project.org/package=GOplot) [12]. Treemaps were created using REVIGO webtool (http://revigo.irb.hr/index.jsp) [13]. Gene enrichment analysis was performed using DAVID 2010 Bioinformatics Resources (http://david.abcc.ncifcrf.gov/) [14].

Reverse transcription and real-time quantitative PCR

Using the PrimeScript II 1st strand cDNA Synthesis Kit (Takarabio, Japan), 3 micrograms of total RNA were transformed into first-strand complementary DNA synthesis following directions provided by the manufacturer. Human pre-messenger RNA sequences were obtained from NCBI gene (www.ncbi.nlm.nih.gov/gene/) before using NCBI blast (https://blast.ncbi.nlm.nih.gov/Blast.cgi) to design primers in PCR. All the primer sequences used in this study can be checked in Table S1. Real-time quantitative PCR (qPCR) was performed to evaluate the expression levels using SYBR Green Master Rox (Roche, Sigma-Aldrich), and were analyzed using the StepOnePlus real-time system (Applied Biosystems). The endogenous expression level of GAPDH was used to obtain the expression levels of other genes via ΔΔCt methods.

Drug resistance and CCK8 assay

Cells were seeded at the concentration of 1 x 10^4 cells/ml in 96-well plates and incubated overnight before application of various concentration of chemotherapy drugs (1μM to 200μM 5-FU (KYOWA KIRIN, Japan)). After 96 hours, medium was discarded and CCK8 assay solution (Dojindo molecular technologies) was added to cells and incubated for 1 hour at 37°C. The plate was then read by a microplate reader (OD450; Infinite F50, TECAN).

Western blotting assay

Proteins were extracted from relevant cell lines using ice-cold RIPA buffer (Nacalai Tesque, Japan) after washing with 1x phosphate-buffered saline (PBS). Later proteins were separated in 10-20% gels (SuperSep Ace, Fujifilm Wako, Japan) and then transferred onto PVDF membranes (Immobilon-P, Merck M), and blocked using skimmed milk (Fujifilm Wako, Japan). The collection of primary antibodies used in this study were Snail (ab53519; Abcam), CCN3 (ab191425; Abcam), NEFL (ab223343; Abcam), and E-cadherin (24E10, Cell Signaling Technology), Vimentin (D21H3, Cell Signaling Technology), CD24 (ab199140 Abcam). Proteins were incubated with the primary antibodies over night at 4°C. They were then stained with anti-mouse, anti-rabbit or anti-goat secondary antibodies (Jackson Laboratory) for 60 minutes at room temperature. Thereafter they were incubated with chemiluminescent HRP substrate (WBKLS0500, Merck M) for 5 minutes. Chemiluminesence signals were collected via the Fujifilm LAS-3000 (Fuji, Japan) as per the manufacturer's instructions.

Immunocytochemistry and fluorescence assay

Cells were seeded onto 8-well culture slides (#354118, Falcon) overnight before fixation with 4% PFA for 10 minutes at room temperature followed by 1x PBS washes. Cells were permeabilized with 0.5% Triton X-100/PBS for 5 minutes at room temperature, washed with 1x PBS, and blocked in 5% BSA (Sigma) in PBS for 60 minutes before incubating with Snail (20C8, ThermoFisher) primary antibodies followed by the secondary antibodies Alxea Fluor 594 (ThermoFisher). Slides were mounted in VECTASHIELD Mounting Medium with DAPI (H-1200; VECTOR Lab, Japan). Fluorescence images were visualized with Keyence fluorescence microscope.

Immunohistochemistry staining

Human gastric cancer tissue array (MLB Life Science Japan) and tumor specimens from mice gastric tumors were deparaffinized, rehydrated and placed in 3% (v/v) H_2O_2–methanol for 15 min at room temperature. The slides were then immersed in blocking solution (Non-specific Staining Blocking Reagent; Dako-Cytomation, Kyoto, Japan) for 15 min and incubated with the primary antibodies listed below at 4 ^{0}C overnight. Antigen–antibody complexes were detected with a secondary antibody (Histofine Simple Stain MAX PO (R) for rabbit monoclonal, or (G) for goat polyclonal (Nichirei, Tokyo, Japan) and visualized using 3,30-diaminobenzidine (0.5 mg/ml in Tris-buffered saline). The list of primary antibodies and dilution ratios were as follows: 1. Anti-SNAIL antibody (goat polyclonal, ab53519, Abcam), 1: 1,000; 2. Anti-CCN3 antibody (rabbit monoclonal, ab191425, Abcam), 1:100; 3. Anti-NEFL antibody (rabbit monoclonal, ab223343, Abcam), 1:400.

Flow cytometry

Incubation buffer was prepared as 1x PBS + 2% FBS. Single cell suspensions were washed with cooled incubation buffer, and re-suspended in 1x PBS + 2% FBS on ice for 30 minutes for antibody blocking: anti-CD24-FITC (ML5; Bio-legend, San Diego, CA), CD44-FITC (BJ18; Bio-legend, San Diego, CA) and DAPI (422801, Bio-legend, San Diego, CA). Cells were suspended in 0.5 mL incubation 1x PBS + 2% FBS to reach a final concentration of 10^6 cells/ml. Data were collected by the BD FACSCanto II or BD FACSVerse flow cytometer (Becton-Dickinson, Franklin Lakes, NJ) and analyzed with FlowJo software (TreeStar, San Carlos, CA). Cell debris was excluded from the analysis based on scatter signals, and fluorescent compensation was adjusted when double stained.

Statistical Analyses

Independent sample t tests were performed to compare the continuous variation of two groups, and the student's test was applied for comparisons of variables. $P < 0.05$ was considered significant. All data are reported as mean ±SEM.

Results

Gastric Spheres Cultured Under Serum-Free Conditions Manifest Stem Cell Properties

Self-renewal capability is a major property of stem cells, and can be accurately assessed via sphere formation [15]. Gastric cancer cell lines produce stem like sphere-forming cells when cultured under B-27(+) bFGF(+) EGF(+) serum-free medium (CSC serum-free medium) in ultra-low attachment culture dishes [16]. The original gene expression profiles and tumor morphologies in cancer cells are well reflected with spheres cultured in the CSC serum-free condition [17]. We assessed the sphere-forming capacity of five gastric cancer cell lines for initial culture (cells were collected from attached condition and seeded in CSC serum-free medium) and passage culture (cells were collected from formed spheres and seeded in CSC serum-free medium), and found that three cell lines had the ability to form spheres (Figure 1A). Those spheres all originated from single cell and not by mere cell herds or aggregations, which was ensured by seeding single cells in 96 well plates and spheres managed to develop after several weeks (data not shown). Sphere-forming capacity of passaged cells (passage culture) was stronger compared with that of parental cells (initial culture), when the same number of cells were seeded in CSC serum-free medium (Figure 1B). To further confirm whether malignant cells possess additional stemness traits, 1 x 10^4 NCI-N87 cells were transplanted into the flanks of NOD/SCID mice. Histological analysis of xenografts exhibited an epithelial-like morphology irrespective of whether they were generated by parental or sphere cells (Figure 1C & S1);

however, sphere cells were more efficient at producing bulky tumors in NOD/SCID mice compared with parental monolayer cells (Figure 1D).

Gastric Spheres Express EMT-associated Factors

Acquisition of stemness traits in malignant cells is commonly achieved through undergoing EMT process, thus tracking the activities of EMT-associated factors will help uncovering mechanism behind the obtained stemness. Four key EMT factors were examined in this study, and higher mRNA expression of EMT factors (TWIST1, 2, SNAIL, and SLUG) were found in spheres compared with parental cells (Figure 2A). HGC27 cells, which form spheres most efficiently, highly expressed TWIST1 and SNAIL mRNAs compared with other two sphere-forming cell lines, NCI-N87 and NUGC3. Consistent with this, immunofluorescence images indicated highest protein expression of SNAIL in HGC27 cells (Figure 2B). The role of TWIST1 has been extensively investigated in previous EMT-associated researches [18]; therefore, HGC27 and SNAIL were chosen as the target cell line and molecule pair in the current study.

SNAIL Regulates Tumorigenicity in Gastric Cancer Cells

In order to investigate whether SNAIL regulates stemness and tumorigenicity in gastric spheres, we determined phenotypic alteration after lentivirus-mediated short-hairpin RNA-interfered knockdown of SNAIL (shRNA-SNAIL k.d.). Realtime quantitative PCR

indicated successful knockdown effects using shRNA-SNAIL in HGC27 cell lines and spheres (Figure 3A). Western blotting showed a similar tendency of 29 Da SNAIL protein expression (Figure 3B). Epithelial and mesenchymal traits of HGC27 were measured using antibodies against E-cadherin and Vimentin, representative proteins for epithelial and mesenchymal phenotypes, respectively. Up-regulation of E-cadherin with down-regulation of Vimentin by SNAIL knockdown indicated the event of mesenchymal-to-epithelial transition in HGC27 cell lines (Figure 3B). The most conspicuous phenomenon observed was that the shape of formed sphere in the CSC serum-free medium switched from having smooth margins into jagged and sharp edges by the SNAIL knockdown (Figure 3C). Previous studies reported a CD44+/CD24– subpopulation of gastric cancer contains gastric cancer stem cells [19]. As showed in Figure 3D, the fluorescence activated cell sorter analysis revealed that 91.0% of the HGC27 cell line was CD44+/CD24–, while knockdown of SNAIL in this cell line almost completely eliminates this population. This suggested that gastric cancer stem cells are maintained, at least in part, by the presence of SNAIL.

Stemness such as self-renewability in cancer cells is associated with the capacity of forming spheres out of the transformed epithelial cells [20]. Therefore, we compared sphere forming capacity between parental HGC27 and stable SNAIL knockdown HGC27 cells cultured in monolayer conditions. The number and area of sphere were significantly decreased by SNAIL knockdown, suggesting a reduced ability to self-renewal (Figure 3E). Consistent with this, when 1 x 10^4 cells were transplanted into the flanks of NOD/SCID mice, although histological analysis did not show any significant alterations, stably SNAIL

knockdown HGC27 cells were less efficient at producing bulky tumors compared with parental HGC27 cells (Figure 3F).

Lower expression of SNAIL was referred to as increased sensitivity upon chemo-treatment due to diminished self-renewability in malignancy [21]. In our experimental condition, stable SNAIL knockdown HGC27 cells were more susceptible to 5-fluorouracil (5-FU) treatment compared with parental HGC27 cells (Figure 3G).

Together, these findings SNAIL regulates tumorigenecity, possibly stemness at least in part, in gastric cancer cells.

SNAIL-regulating Genes in Gastric Cancer Cells

To unveil the mechanisms underlying phenotypic modifications induced by knockdown of SNAIL in HGC27 cells, gene expression microarray analysis on a HGC27-SNAIL knockdown and parental HGC27 cells was performed. Under the alteration of SNAIL expression, distributed genes movement were shown in Figure 4A. Of those genes, a total of 1656 and 1832 probe sets ($|FC| \geq 2$) were specifically upregulated or downregulated in stable HGC27-SNAIL knockdown cells respectively (Figure 4B). Statistically overrepresented functional processes were obtained through enriched genes querying in the Gene Ontology (GO) database ($P < 0.05$; Figure 4C). The main processes enriched in up-/down-regulated genes include those pertaining to multiple binding and cellular processes. It is suggested that instead of individual activation, genes tend to

collaborate in genetic networks, thus we subjected the enriched GO processes that were selected as meaningful to REVIGO analysis, which is a useful web tool that summarizes long lists of GO terms. Several GO terms formed a treemap of the most significant processes: cell motility, chemotaxis, adhesion, neural regeneration, and cell death, as well as those involved in EMT (Figure 4D). Within this network, chemotaxis was a focal node and in the broader group of terms under the chemotaxis title, the regeneration process was chosen as a target to be studied in greater depth due to the possible role of neuron development and supervision in malignancy progression. qRT-PCR confirmed down- and up-regulation of CCN3 (also known as NOV or IGFBP9): Cellular Communication Network factor 3, and NEFL: Neurofilament Light peptide mRNA expression by SNAIL knockdown in HGC27cells (Figure 4E).

CCN3 and NEFL Expression in Gastric Cancers

The occurrence of distant metastases and poor survival outcome has been reported relevant with high SNAIL protein in gastric cancer patients [22]. CCN3 belongs to the CCN family (cysteine-rich protein 61 (**C**YR61), connective tissue growth factor (**C**TGF), nephroblastoma overexpressed (**N**OV)). Limited information is known concerning the functional correlation between EMT with CCN3 and NEFL in cancers. There have been reports of increased expression of CCN3 in prostate and cervical cancers [23, 24]. CCN3 was demonstrated to promote EMT by activating the FAK/Akt/HIF-1α pathway in prostate cancer [25]. NEFL has been implicated in carcinogenesis as a putative suppressor gene in

neuron related inhibition of both cell proliferation and invasion in head and neck squamous cell carcinoma [26]. Using data of transcript level of SNAIL, CCN3 and NEFL from The Cancer Genome Altas (TCGA) stomach adenocarcinoma project, each gene expression in gastric cancers and normal gastric tissues were shown in Figure 5A. There were no correlations in mRNA expression levels between SNAIL and either CCN3 or NEFL, and no correlation between CCN3 and NEFL (Figure 5B). Immunohistochemistry analysis was then performed on a paraffin-embedded human gastric cancer tissue array (n = 30, purchased from MBL Life Science, Japan). CCN3 expression was detected in 96.7% (29/30), NEFL expression was positive in 86.7% (26/30) and SNAIL expression occurred in 26.7% of tumor tissues (8/30). Representative staining with positive and negative images for SNAIL/CCN3/NEFL are shown in Figure 5C. Compared with Figure S2 of normal gastric tissues, CCN3 antibody only stained positive in some fibroblasts and myofibroblasts besides malignant parts; while NEFL also stained positive in neurofilament as reported elsewhere.

CCN3 and NEFL are Critical for SNAIL-Induced Stemness

We initially investigated how CCN3 and NEFL function by introducing their expression vectors into SNAIL knockdown HGC27 cells and parental HGC27 cells respectively, and those effects were confirmed with western blotting (Figure 6A). Forced expression of SNAIL or CCN3 in sh-SNAIL knockdown HGC27 cells resulted in significantly increased number of formed spheres (Figure 6B-a & b); while that of NEFL

caused diminished sphere formation ability in parental HGC27 cells (Figure 6B-c). Furthermore, the chemoresistance against 5-FU of each pair of cells was also measured. The results were consistent with alterations to sphere formation capacity: the proliferation rates of HGC27-shSNAIL, HGC27-NEFL, and HGC27-shSNAIL-CCN3 cells were reduced more rapidly when 5-FU was added in a dose-dependent manner (Figure 6C). The fact that HGC27-shSNAIL stable knockdown cells produced significantly reduced tumor masses compared with SNAIL re-introduced rescue cells was proved via xenograft assays in vivo (data not shown). To further evaluate the role of NEFL molecule during EMT process, gastric cancer cell line IM95 was selected from several candidate cell lines due to high NEFL expression level. Several observations can be witnessed after knockdown of NEFL in IM95: steady knockdown of NEFL using shRNA in IM95 cell was established and verified (Figure 6D-a & b), with enhanced mesenchymal and decreased epithelial indexes of vimentin and E-cadherin discovered from knockdown of NEFL respectively (Figure 6D-b), and increased chemo-resistance effect throughout proliferation assay with 5FU addition as well (Figure 6D-c).

Discussion

In this study, we established three spheres enriched in CD44+ gastric cancer cells. The spheres displayed EMT phenotype, high tumorigenecity, and chemoresistance against 5-FU treatment. SNAIL, one of the key regulators of EMT, was upregulated in the spheres, and CCL3 and NEFL were further extracted as downstream targets of SNAIL by microarray analyses. Re-introduced expression of CCN3 and NEFL partially impaired the SNAIL-dependent CSC like activity, tumorigenicity, and chemoresistance in HGC-27 gastric cancer cells, rescpectively.

Previous studies have uncovered that CD44, EPCAM, CD133, CD24, CD166 or Aldh are CSC markers in certain circumstances and are enriched in spheres generated from gastric cancer cell lines or clinical tissues [27, 28]. Although it stills opens to be discussed whether all CD44+ cells are CSCs, the CD44+ subpopulation is reported to previal in cancer cells after spheres are formed. In this study, we also showed that the CD44+ subpopulation was enriched in gastric spheres.

In a mammospheres formation assay, expression of EMT-associated factors, such as TWIST1/2, SNAIL, and SLUG in breast cancer cells are up-regulated and associated with the acquisition of CSC properties and greater metastatic ability after EMT process [29]. These EMT-associated molecules are involved in multiple signaling pathways in other types of cancers. In the present study, expression of TWIST1 and SNAIL were significantly elevated in gastric spheres, especially in HGC27-derived spheres. The role of TWIST1 in EMT processes during gastric carcinogenesis has been extensively investigated [30, 31],

while that of SNAIL has not been researched as much as TWIST1. Therefore, we focused on the functional analyses of SNAIL and its downstream targets in gastric carcinogenesis. Indeed, we showed that knockdown of SNAIL resulted in acquisition of EMT-phenotype and loss of CD44+ cell population. It also led to the impaired growth of gastric cancer xenografts and chemoresistance against 5-FU treatment. These data are consistent with discoveries reported in other solid malignancies [32-34], and indicates crucial roles of SNAIL in regulating CSC properties.

To further explore the underlying mechanisms of SNAIL-mediated gastric carcinogenesis, we performed microarray analyses which revealed transcriptome alterations by knockdown of SNAIL. GO terms formed a treemap of the most significant processes: cell motility, chemotaxis, adhesion, neural regeneration, and cell death, as well as those involved in EMT. Among the components from the network of chemotaxis, for example, sox2 has been reported as the key regulator in CSCs and is over expressed in various tumors. Other significant genes included TGFB1 and NOTCH1; both belong to the Notch signaling pathway, which plays an important role in angiogenesis and CSC self-renewal [35]. Indeed, most of the significant GO terms identified are implicated in well-known signaling processes. Genes from the regeneration process were also included in EMT process with significant biological functions. Among them, CCN3 is described in prostate cancer [23]. Meanwhile, NEFL, was found to be expressed in a wide range of malignancies as a tumor suppressor gene [36]. Based on study interest, CCN3 and NEFL were here chosen as two possible downstream targets of SNAIL that seem to function in stemness in gastric cancer.

CCN3 belongs to the three-member family of cysteine-rich regulatory proteins and has been found in various cancer cells and surrounding tissues, suggesting that in the cancer microenvironment, it is likely that CCN3 may act as a EMT-regulatory factor [37]. Consistent with this, CCN3 requires its C-terminal domain for bone metastatic function, and is correlated with aggressive disease progression in prostate cancer [38]. In hepatocellular carcinoma, after being secreted from hepatic cells, CCN3 gained its' activity in various processes during EMT via HSCs (Hepatic stellate cells) [39]. A previous study has also shown that increased expression level of CCN3 expression lead to local invasion and distant metastases in gastric cancer [40, 41]. In this study, we showed that a link between CCN3 expression and gastric stemness properties, and have further shown that low levels of CCN3 in HGC27 cells result in reduced stemness and tumorigenicity. Therefore, approaches that capable of reducing CCN3 expression have the potential to suppress EMT and to be novel therapies against gastric cancer.

NEFL, which practically maintains the neuronal caliber and functions as a regulator in intracellular transport to axons and dendrites, has also be implicated in various carcinogenesis [42]. NEFL acts as a tumor suppressor in non-small cell lung cancer (NSCLC), inhibiting invasion and metastasis, while methylation may destroy its protective effect [43]. In NSCLC and breast cancer, patients with higher expression of NEFL mRNA transcript had a better five-year disease-free survival [36]. In contrast to these reports, our study showed that NEFL might enhance the tumor development in xenografts. The reason behind the contrasting outcomes maybe due to the fact that in the advanced stage of malignancy, cancer cells tend to become much fiercer in metastatic potential and

phenotypes, thus the invasions are nowhere to be hold arrested by merely cytoprotective genes expression alterations [44]. In either case, NEFL in digestive system cancers such as gastric cancer may play distinct roles in a context-dependent manner.

In conclusion, we showed that SNAIL regulates the expressions of CCN3 and NEFL genes in human gastric cancer cells, and that these in turn control the CSC activities. Strategies that disrupt this possible circle may be possible to treat gastric cancer in future. Double antagonists targeting both CCN3/NEFL-SNAIL axis may weaken the malignant progression and dual RNAi study should be considered before RNAi compound development. Also, protein secretion of the target molecule that plays important roles in malignancy can be traced and intentionally attacked through clonal antibody. Multiple channels of further application as therapeutic agents may be helpful for patients with gastric cancer.

Competing Interests:

We have received research funds under contract from Sumitomo Danippon Pharma Co., Ltd.

Acknowledgement:

The authors thank M Nishikawa, Kyoto Institute of Nutrition & Pathology, Inc., and K Kokuryo, the Center for Anatomical, Pathological and Forensic Medical Research, Kyoto University Graduate School of Medicine, for immunohistochemistry staining.

References:

1. Rawla P, Barsouk A.Epidemiology of gastric cancer: global trends, risk factors and prevention. Prz Gastroenterol. 2019; 14: 26–38.

2. Afify SM, Seno M. Conversion of stem cells to cancer stem cells: undercurrent of cancer initiation. Cancers (Basel). 2019; 11: 345.

3. Jolly MK, Celià-Terrassa TDynamics of phenotypic heterogeneity associated with EMT and stemness during cancer progression. J. Clin. Med. 2019, 8, 1542.

4. Hollier BG, Tinnirello AA, Werden SJ, Evans KW, Taube JH, Sarkar TR, et al. Tinnirello, FOXC2 expression links epithelial-mesenchymal transition and stem cell properties in breast cancer. Cancer Res. 2013; 73: 1981–1992.

5. Mani SA, Guo W, Liao MJ, Eaton EN, Ayyanan A, Zhou AY,et al. The epithelial-mesenchymal transition generates cells with properties of stem cells. Cell. 2008; 133: 704–715.

6. Guen VJ, Chavarria TE, Kröger C, Ye X, Weinberg RA, Lees JA. EMT programs promote basal mammary stem cell and tumor-initiating cell stemness by inducing primary ciliogenesis and Hedgehog signaling. PNAS. 2017; 114: E10532–E10539.7. Wang Y, Shi J, Chai K, Ying X, P Zhou B. The role of snail in EMT and tumorigenesis. Curr Cancer Drug Targets. 2013; 13: 963–972.

7. Cristina Peña, José Miguel García, Javier Silva, Vanesa García, Rufo Rodríguez, Isabel Alonso, et al. E-cadherin and vitamin D receptor regulation by SNAIL and ZEB1 in colon cancer: clinicopathological correlations. Human Molecular Genetics. 2005; 14: 3361–3370.

8. Brzozowa M, Michalski M, Wyrobiec G, Piecuch A, Dittfeld A, Harabin-Słowińska M, et al. The role of Snail1 transcription factor in colorectal cancer progression and metastasis. Contemp Oncol (Pozn). 2015; 19: 265–270.

9. Serrano-Gomez SJ, Maziveyi M, Alahari SK. Regulation of epithelial-mesenchymal transition through epigenetic and post-translational modifications. Mol Cancer. 2016; 15: 18.

10. Tusher VG, Tibshirani R, Chu G.Significance analysis of microarrays applied to the ionizing radiation response.Proc Natl Acad Sci USA. 2001; 98 (9): 5116–5121.

11. Gautier L, Cope L, Bolstad BM, Irizarry RA. affy—analysis of Affymetrix GeneChip data at the probe level. Bioinformatics. 2004 12; 20: 307–315.25. Huang DW, Sherman BT, Lempicki RA.Systematic and integrative analysis of large gene lists using DAVID Bioinformatics Resources. Nature Protoc. 2009; 4: 44–57.

12. Walter, Wencke, Fatima Sanchez-Cabo, and Mercedes Ricote. GOplot: an R package for visually combining expression data with functional analysis. Bioinformatics. 2015; 31: 2912-2914.

13. Fran Supek ,Matko Bošnjak,Nives Škunca,Tomislav Šmuc. REVIGO Summarizes and Visualizes Long Lists of Gene Ontology Terms. PLoS ONE. 2011 July 18.

14. Huang DW, Sherman BT, Lempicki RA. Bioinformatics enrichment tools: paths toward the comprehensive functional analysis of large gene lists. Nucleic Acids Res. 2009; 37: 1–13.

15. Al-Hajj M, Clarke MF. Self-renewal and solid tumor stem cells. Oncogene. 2004; 23: 7274–82.28. Ni SJ, Zhao LQ, Wang XF, Wu ZH, Hua RX, Wan CH, et al. CBX7 regulates stem cell-like properties of gastric cancer cells via p16 and AKT-NF-κB-miR-21 pathways. J Hematol Oncol. 2018; 11: 17.

16. Seon Ok Min, Sang Woo Lee, Seon Young Bak, Kyung Sik Kim. Ideal sphere-forming culture conditions to maintain pluripotency in a hepatocellular carcinoma cell lines. Cancer Cell Int. 2015; 15:95.

17. Ishiguro T, Ohata H, Sato A, Yamawaki K, Enomoto T, Okamoto K. Tumor-derived spheroids: Relevance to cancer stem cells and clinical applications. Cancer Sci. 2017; 108: 283–289.

18. Chang Ohk Sung, Keun-Woo Lee, Songying Han, and Seok-Hyung Kim. Twist1 Is Up-Regulated in Gastric Cancer-Associated Fibroblasts with Poor Clinical Outcomes. Am J Pathol. 2011; 179: 1827–1838.

19. Takaishi S, Okumura T, Tu S, Wang SS, Shibata W, Vigneshwaran R, et al. Identification of gastric cancer stem cells using the cell surface marker CD44. Stem Cells. 2009; 27: 1006–1020.

20. Lim S, Becker A, Zimmer A, Lu J, Buettner R, Kirfel J. SNAI1-mediated epithelial-mesenchymal transition confers chemoresistance and cellular plasticity by regulating genes involved in cell death and stem cell maintenance. PLoS ONE. 2013; 8.

21. Smith, Bethany N, and Valerie A Odero-Marah. The role of Snail in prostate cancer. Cell adhesion & migration. 2012; 6: 433-41.

22. Klaudia Skrzypek, Marcin Majka. Interplay among SNAIL Transcription Factor, MicroRNAs, Long Non-Coding RNAs, and Circular RNAs in the Regulation of Tumor Growth and Metastasis. Cancers. 2020; 12:1.

23. Maillard M, Cadot B, Ball RY, Sethia K, Edwards DR, Perbal B, et al. Differential expression of the ccn3 (nov) proto-oncogene in human prostate cell lines and tissues. Mol Pathol. 2001; 54: 275–280.

24. Zhang T, Zhao C, Luo L, Xiang J, Sun Q, Cheng J, et al. The clinical and prognostic significance of CCN3 expression in patients with cervical cancer. Adv Clin Exp Med. 2013; 22: 839–45.

25. Chen PC, Tai HC, Lin TH, Wang SW, Lin CY, Chao CC, et al. CCN3 promotes epithelial-mesenchymal transition in prostate cancer via FAK/Akt/HIF-1α-induced twist expression. Oncotarget. 2017; 8: 74506–74518.

26. Huang Z, Zhuo Y, Shen Z, Wang Y, Wang L, Li H, et al. The role of NEFL in cell growth and invasion in head and neck squamous cell carcinoma cell lines. J Oral Pathol Med. 2014; 43:191–198.

27. Phu Hung Nguyen, Julie Giraud, Lucie Chambonnier, Pierre Dubus, Linda Wittkop, Geneviève Belleannée, et al. Characterization of Biomarkers of Tumorigenic and Chemoresistant Cancer Stem Cells in Human Gastric Carcinoma. Clin Cancer Res. 2017; 23: 6.

28. Xiao-Long Chen, Xin-Zu Chen, Yi-Gao Wang, Du He, Zheng-Hao Lu, Kai Liu, et al. Clinical significance of putative markers of cancer stem cells in gastric cancer: A retrospective cohort study. Oncotarget. 2016; 7: 38.

29. I. K. Guttilla, K. N. Phoenix, X. Hong, J. S. Tirnauer, K. P. Claffey, B. A. White. Prolonged mammosphere culture of MCF-7 cells induces an EMT and repression of the estrogen receptor by microRNAs. Breast Cancer Res Treat. 2012; 132:75–85.

30. Jianxin Qian, Yizhou Luo, Xiaoqiang Gu, Wang Zhan, and Xi Wang. Twist1 Promotes Gastric Cancer Cell Proliferation through Up-Regulation of FoxM1. PLoS One. 2013; 8: e77625.

31. Rosivatz E, Becker I, Specht K, Fricke E, Luber B, Busch R, Höfler H, Becker KF. Differential expression of the epithelial-mesenchymal transition regulators snail, SIP1, and twist in gastric cancer. Am J Pathol. 2002; 161: 1881-91.

32. Arti Yadav, Bhavna Kumar, Jharna Datta, Theodoros N. Teknos, and Pawan Kumar. IL-6 promotes head and neck tumor metastasis by inducing epithelial-mesenchymal transition via the JAK-STAT3-SNAIL signaling pathway. Mol Cancer Res; 2011; 9.

33. Cornelia Kröger, Alexander Afeyan, Jasmin Mraz, Elinor Ng Eaton, Ferenc Reinhardt, et al. Acquisition of a hybrid E/M state is essential for tumorigenicity of basal breast cancer cells. PNAS. 2019; 116: 7353-7362.

34. Osorio, L. A., Farfán, N. M., Castellón, E. A., Contreras, H. R. SNAIL transcription factor increases the motility and invasive capacity of prostate cancer cells. Molecular Medicine Reports. 2016; 13: 778-786.

35. Venkatesh V, Nataraj R, Thangaraj GS, Karthikeyan M, Gnanasekaran A, et al. Targeting Notch signaling pathway of cancer stem cells. Stem Cell Investig. 2018; 5: 5.

36. Li XQ, Li L, Xiao CH, Feng YM. NEFL mRNA Expression Level Is a Prognostic Factor for Early-Stage Breast Cancer Patients. PLOS One. 2012; 7: e31146.

37. Kim H, Son S, Shin I. Role of the CCN protein family in cancer. BMB Rep. 2018; 51: 486–492.

38. Dankner M, Ouellet V, Desreumaux-Communal L, Schmitt E, Perkins D, Annis MG, et al. CCN3 is a prognostic biomarker and functional mediator of prostate cancer bone metastasis. AACR; Cancer Res 2019;79.

39. Li W, Liao X, Ning P, Cao Y, Zhang M, Bu Y, et al. Paracrine effects of CCN3 from non-cancerous hepatic cells increase signaling and progression of hepatocellular carcinoma. BMC Cancer. 2019; 19: 395.

40. Li J, Gao X, Ji K, Sanders AJ, Zhang Z, Jiang WG, et al. Differential expression of CCN family members CYR611, CTGF and NOV in gastric cancer and their association with disease progression. Oncol Rep. 2016; 36: 2517–2525.

41. Tsu-Yao Cheng, Ming-Shiang Wu, Kuo-Tai Hua, Min-Liang Kuo, Ming-Tsan Lin, et al. Cyr61/CTGF/Nov family proteins in gastric carcinogenesis. World J Gastroenterol. 2014; 20: 1694-1700.

42. Yuan A, Rao MV, Veeranna, Nixon RA. Neurofilaments at a glance. J Cell Sci. 2012; 125: 3257–3263.

43. Shen Z, Chen B, Gan X, Hu W, Zhong G, Li H, et al. Methylation of neurofilament light polypeptide promoter is associated with cell invasion and metastasis in NSCLC. Biochem Biophys Res Commun. 2016; 470: 627-634.

44. Yokota J. Tumor progression and metastasis. Carcinogenesis. 2000; 21: 497-503.

Legends:

Figure 1. Characteristics of gastric cancer cell lines spheres cultured under serum-free condition.

A. Photographic pictures of sphere morphology.

Initial and passage sphere assay were shown in upper and lower lane pattern respectively with each cell line marked on top.

B. Sphere formed per $2x10^4$ seeded cells as an index of cell renewal capacity.

a: sphere count; b: volume summary of sphere formed. Results were expressed as mean ± SD, * $p<0.05$; ** $p<0.01$.

C. Enhanced in vivo tumor volume formed from spheres in mice at an injection concentration of 4×10^4 cells.

D. Representative H&E slides from gastric cancer cell line NCI-N87 with their sphere formed tumors. Scale bar=200μm.

Figure 2. Stem cell properties and tumor malignancy in gastric cancer spheres.

A. Comparison of EMT factors on absolute mRNA expression levels in gastric cancer cell lines.

B. Immunofluorescence of SNAIL expression in HGC27, IM95 and FU97 cell lines.

a. Cells in the gastric cancer cell lines were found to express SNAIL (imaged with red fluorescent) in the nuclei;

b. Image with DAPI to identify the nuclei of gastric cancer cells;

c. Merged image superimposed on a differential interference contrast background confirms co-localization. Scale bar=50μm.

Figure 3. SNAIL is sufficient and essential for induction of self-renewal and malignancy in gastric cancer cell line HGC27. (Knockdown is represented as k.d.).

A. Real-time quantitative PCR validation of SNAIL expression level in HGC27 and its stable SNAIL knockdown cell lines.

B. Effects of SNAIL knockdown on the expression of E-cadherin and Vimentin in HGC27 cell line.

C. Morphology alteration of gastric cancer cell line HGC27 after SNAIL knockdown in ultra-low attachment condition.

D. CD24 and CD44 FACS profiles of HGC27 and HGC27 SNAIL knockdown cell lines.

E. Sphere formed per $2x10^4$ seeded cells from HGC27 and HGC27 SNAIL knockdown cell.

F. Diminished in vivo tumorigenicity formed from HGC27 SNAIL knockdown cells in NOD/SCID mice at an injection concentration of $4x10^4$ cells. H&E staining of representative tumors, scale bar=200μm.

G. Decreased chemoresistance of HGC27 SNAIL knockdown cells compared with HGC27 when treated with 5-FU.

Figure 4. Microarray analysis between HGC27 and its SNAIL knockdown samples.

A. Plot analysis of distribution visualization of differentially expressed genes comparing SNAIL knockdown and control groups.

B. Bar plot detailing presented numbers of genes under SNAIL up/down regulation in two conditions.

C. GO terms enrichment analysis of molecular function, cellular component and biological process of differentially expressed genes (left to right).

D. The KEGG enrichment analysis of differentially expressed genes.

E. Real-time quantitative PCR validation of CCN3 and NEFL expression level in HGC27 and its stable SNAIL knockdown cell lines.

Figure 5. Elevated expression of SNAIL and CCN3 in patients with stomach adenocarcinoma.

A. mRNA transcript expression levels of SNAIL (a), CCN3 (b) and NEFL (c) are elevated in patients with gastric cancer from TCGA-STAD database. Box in red: malignant tissue; box in blue: normal tissue.

B. No correlation existed between CCN3 and NEFL in gastric cancer patients from TCGA-STAD database.

C. SNAIL, CCN3 and NEFL are highly expressed in human gastric cancer tissues.

Representative immunohistochemical staining (IHC) images of SNAIL, CCN3 and NEFL in gastric cancer tissues. Scale bar = 50 μm.

Figure 6. CCN3 and NEFL correlate with self-renewal and chemoresistance traits in gastric cancer cells.

A. Western blotting analysis of NEFL and CCN3 expression in associated cell lines.

B. Sphere formed per $2x10^4$ seeded cells as an index of cell renewal capacity.

a. HGC27 SNAIL knockdown vs. HGC27 SNAIL knockdown with SNAIL re-introduction;

b. HGC27 vs. HGC27 with NEFL introduction;

c. HGC27 SNAIL knockdown vs. HGC27 SNAIL knockdown with CCN3 re-introduction.

C. Chemoresistance alteration of SNAIL (a), CCN3 (b) and NEFL (c) introduction into associated HGC27 cell lines when treated with 5-FU. Results are expressed as mean ± SD, * $p<0.05$; ** $p<0.01$.

D. Knockdown of NEFL promoted the mesenchymal traits in gastric cancer cell line IM95.

a. Real time qPCR validation of NEFL expression level in IM95 and its stable NEFL knockdown cell lines.

b. Effects of NEFL knockdown on the expression of E-cadherin and Vimentin in IM95 cell line.

c. Increased chemoresistance of IM95 NEFL knockdown cells compared with IM95 cells when treated with 5-FU. Results are expressed as mean ± SD, * $p<0.05$; ** $p<0.01$.

Figure S1. Enhanced in vivo tumor volume formed from spheres in mice at an injection concentration of 4 x 10^4 cells of HGC27 and NUGC3 cells. Representative H&E slides from gastric cancer cell lines with their sphere formed tumors. Scale bar=200μm.

Figure S2. Representative immunohistochemical staining (IHC) images of CCN3 and NEFL in gastric normal tissues. Scale bar = 50 μm.

SNAIL regulates gastric carcinogenesis through CCN3 and NEFL

Role of SNAIL/CCN3/NEFL axis in gastric cancer

Ru Chen[1,2], Kenji Masuo[1,2], Akitada Yogo[1,3], Shoko Yokoyama[1], Aiko Sugiyama[1], Hiroshi Seno[1,2], Akihiko Yoshizawa[4], Shigeo Takaishi[1,*]

1: DSK Project, Medical Innovation Center, Graduate School of Medicine, Kyoto University, Kyoto, Japan.

2: Department of Gastroenterology and Hepatology, Graduate School of Medicine, Kyoto University, Kyoto, Japan.

3: Department of Hepato-Biliary-Pancreatic Surgery and Transplantation, Graduate School of Medicine, Kyoto University, Kyoto, Japan.

4: Department of Diagnostic Pathology, Kyoto University Hospital, Kyoto, Japan.

*Corresponding author: Shigeo Takaishi; takaishi.shigeo.7w@kyoto-u.ac.jp

Abstract

Among cancer cells, there are specific cell populations of whose activities are comparable to those of stem cells in normal tissues, and for whom the levels of cell dedifferentiation are reported to correlate with poor prognosis. Information concerning the mechanisms that modulate the stemness-like traits of cancer cells is limited. Therefore, we here examined five gastric cancer cell lines and isolated gastric oncospheres from three gastric cancer cell lines. The gastric cancer cells that expanded in the spheres expressed relatively elevated proportion of CD44, which is a marker of gastric cancer stem cells, and displayed many properties of cancer stem cells, for example: chemoresistance, tumorigenecity and epithelial-mesenchymal transition (EMT) acquisition. SNAIL, which is a key factor in EMT, was highly expressed in the gastric spheres. Microarray analysis in gastric cancer cell line HGC27 showed that CCN3 and NEFL displayed the greatest differential expression by knocking down of SNAIL; the former was up-regulated and the latter down-regulated, respectively. Down-regulation of CCN3 and up-regulation of NEFL gene expression impaired the SNAIL-dependent EMT activity: high tumorigenicity and chemoresistance in gastric cancer cells. Thus, approach that disrupts SNAIL/CCN3/NEFL axis may be credible in inhibiting gastric cancer development.

Keywords: Gastric Cancer; Cancer Stem Cells; EMT; spheroid

Introduction

Gastric cancer is one of the most common cancers in East Asia and Eastern Europe [1]. It is importan~~eet~~ to critically assess the current advances in our understanding of gastric cancer and to establish novel and innovative therapeutic strategies. A vast body of literature has been published on specific aspects of cancer initiating cells and on putative cancer stem cells (CSCs) which possess properties of stem cells distinct from differentiated progeny cancer cells [2]. Discovering significant genes and signaling pathways involving gastric cancer stemness could be helpful approaches to discovering novel therapeutic options.

During malignancy transformation, a critical process named the epithelial-mesenchymal transition (EMT) commonly occurs, and cells usually undergo a rapid change from differentiated and polarized epithelial state into an invasive mesenchymal composition [3]. During the development of diverse solid tumors, stem cell like traits were reported to be related to EMT. For example, after breast cancer cells acquired stem cell like features, the passaged mammosphere cells manifest with similar features to breast cancer stem cells, indicating a fundamental link between malignancy propagation and stem cell characteristics [4-6]. Among all the major EMT transcription factors, SNAIL, a zinc-finger protein, whose activities in relation to the downregulation of E-cadherin in colon cancer have previously been reported [7, 8]; binds to the E-boxes in the *CDH1* gene promoter and represses transcription of the *CDH1* gene [9]. So far, SNAIL has been reported to contribute in many malignancy progression, and its' function in gastric cancer needs to be uncovered further as well. The precise mechanism of SNAIL-induced cell dedifferentiation and how this gene

can provide stem cell like traits in gastric cancer cells remain open to debate and to be further clarified. The discovery of genes under SNAIL regulation that could also be an instrumental breakthrough and lead to the establishment of novel therapeutic strategies in EMT-related stemness and malignancy. In the present study, we extracted CCN3 and NEFL as targets in the downstream of SNAIL, and determined the association of these two factors with stem cell like activity in gastric cancer cells.

Materials and Methods:

Cell culture, tissue collection and sphere growth

Human gastric cancer cell lines were purchased from RIKEN (https://cell.brc.riken.jp/ja/quality/str), JCRB cell bank (https://cellbank.nibiohn.go.jp/about-qc_english/), and ATCC (https://www.atcc.org/Services/Testing_Services/Cell_Authentication_Testing_Service.aspx), in which STR analysis is performed in these cell line banks to ensure the authentication of human cell lines, and were cultured according to the instructions provided by the manufacturer. Cell lines including human gastric cancer cell lines (HGC27, NCI-N87, GSU, MKN74, MKN45 ~~and NUGC3~~, NUGC3 and IM95), and embryonic kidney 293T cells were cultured in DMEM (Nacalai Tesque, Japan) supplemented with 10% fetal bovine serum (HyClone Defined Fetal Bovine Serum (FBS), USA) and penicillin-streptomycin mixed solution (10,000u/ml, Nacalai Tesque, Japan). For RNA extraction from each cell line, NucleoSpin RNA Plus (Takarabio, Japan) was used following the manufacturer's instructions. The preparation of paraffin-embedded blocks was performed as follows: slices of tumor formed from each of the cell lines were immersed in 4% paraformaldehyde (Nacalai Tesque, Japan) to allow the assembling of paraffin-embedded blocks. Cells were cultured in homemade stem cell medium (DMEM/F12 supplemented with B27 Supplement (ThermoFisher), 10 ng/mL recombinant basic fibroblast growth factor (bFGF, ThermoFisher), 10 ng/mL epidermal growth factor (EGF, ThermoFisher), and 1% penicillin-streptomycin) to obtain spheres. A total of 1 x 10^4 cells per milliliter were seeded

in culture medium for stem cell and incubated in ultra-low attachment plates for 5 days. Spheres larger than 80 μm in diameter were counted using Cell3Imager (InSphero AG and Dainippon SCRREEN, Kyoto, Japan). TrypLE Express (ThermoFisher) or Trypsin-EDTA (FUJIFILM Wako, Japan) were used to separate cells from the floating spheres and adherent cells to allow cell counting and other experiments.

In vivo tumorigenicity assay

All procedures involving animals were conducted in accordance with the Institutional Animal Welfare Guidelines of Kyoto University. NOD/SCID mice were purchased from the Charles River Laboratories (Yokohama, Japan) and were maintained according to the Guidelines for Laboratory Animals in the Kyoto University. The tumorigenicity assay was performed by subcutaneous injection of 1 x 10^4 designated cells into the flanks of 8- to 10-week-old NOD/SCID mice. Mice were sacrificed and examined for tumor harvest once the tumor had reached pre-determined size (2.5cm maximum). Tumor size was measured with calipers once a week after the injection.

Lentivirus production, short-hairpin RNA-mediated human SNAIL gene knockdown and stable clone establishment

The lentivirus package system: pMDLg/pRRE (Addgene, plasmid #12251), pRSV-Rev (Addgene, plasmid #12253) and pMD2.G (Addgene, plasmid #12259) together with the shRNA plasmid targeting the human SNAIL gene as well as the control vector: pLKO.1puro (Addgene, plasmid #8453) were co-transfected into 293T cells by Lipofectamine 3000 (Invitrogen). SNAIL-targeting short-hairpin RNA (MISSION shRNA)

duplex (A: 5-TGCTCCACAAGCACCAAGAGTC-3; B: 5-CCACTCAGATGTCAAGAAGTAC-3) and NEFL-targeting short-hairpin RNA (MISSION shRNA) (5-CGACAGCTTGATGGACGAAAT-3) were ~~was~~ purchased from Sigma-Aldrich Co. LCC. (St. Louis, MO, USA). About 48 to 72 hours later, virus supernatant was collected for concentration. For shRNA knockdown, HGC27 cells were seeded onto 6-well plates and infected with optimal virus concentrations supplemented with 6 μg/mL Polybrene (Sigma, St. Louis, MO, USA), then incubated for 12 hours before replacing with fresh medium. Cells were then selected by puromycin (INVIVOGEN, Japan) at the concentration of 1.8 μg/ml (HGC27) and 4 μg/ml (IM95) for 2 weeks.

Transient transfection

Lipofectamine 3000 reagent was used for the introduction of overexpression vectors to establish stable lines, including the NEFL (Sino Biol.HG13214-UT), CCN3 (Sino Biol.HG10264-UT) and SNAIL (Sino Biol.HG16844-UT) overexpression vectors and matched control vector (Sino Biol.CV011), all of which were purchased from Sino Biological Inc. (Wayne, PA, USA). Selections were carried out via hygromycin B (Nacalai Tesque, Japan); resistance and transfection efficiency were verified through real-time qPCR.

Microarray data and bioinformatics analysis

Total RNA from each sample was extracted using NucleoSpin RNA Plus kit, forwarded with Affymetrix Human Genome U133 Plus 2.0 Array (HuGene2.9st, Japan) analysis. RNA extraction, microarray hybridization, and feature selection were performed according to the manufacturer's protocol. Microarray data can be download from the GEO

database (https://www.ncbi.nlm.nih.gov/geo/query/acc.cgi?acc=GSE145867). Bioinformatics and genetic network construction were performed in R Studio (version 1.2.1335) mainly using RMA [10] from the affy package [11] and the GoPlot package (https://CRAN.R-project.org/package=GOplot) [12]. Treemaps were created using REVIGO webtool (http://revigo.irb.hr/index.jsp) [13]. Gene enrichment analysis was performed using DAVID 2010 Bioinformatics Resources (http://david.abcc.ncifcrf.gov/) [14].

Reverse transcription and real-time quantitative PCR

Using the PrimeScript II 1st strand cDNA Synthesis Kit (Takarabio, Japan), 3 micrograms of total RNA were transformed into first-strand complementary DNA synthesis following directions provided by the manufacturer. Human pre-messenger RNA sequences were obtained from NCBI gene (www.ncbi.nlm.nih.gov/gene/) before using NCBI blast (https://blast.ncbi.nlm.nih.gov/Blast.cgi) to design primers in PCR. All the primer sequences used in this study can be checked in Table S1. Real-time quantitative PCR (qPCR) was performed to evaluate the expression levels using SYBR Green Master Rox (Roche, Sigma-Aldrich), and were analyzed using the StepOnePlus real-time system (Applied Biosystems). The endogenous expression level of GAPDH was used to obtain the expression levels of other genes via ΔΔCt methods.

Drug resistance and CCK8 assay

Cells were seeded at the concentration of 1 x 10^4 cells/ml in 96-well plates and incubated overnight before application of various concentration of chemotherapy drugs

(1μM to 200μM 5-FU (KYOWA KIRIN, Japan)). After 96 hours, medium was discarded and CCK8 assay solution (Dojindo molecular technologies) was added to cells and incubated for 1 hour at 37°C. The plate was then read by a microplate reader (OD450; Infinite F50, TECAN).

Western blotting assay

Proteins were extracted from relevant cell lines using ice-cold RIPA buffer (Nacalai Tesque, Japan) after washing with 1x phosphate-buffered saline (PBS). Later proteins were separated in 10-20% gels (SuperSep Ace, Fujifilm Wako, Japan) and then transferred onto PVDF membranes (Immobilon-P, Merck M), and blocked using skimmed milk (Fujifilm Wako, Japan). The collection of primary antibodies used in this study were Snail (ab53519; Abcam), CCN3 (ab191425; Abcam), NEFL (ab223343; Abcam), and E-cadherin (24E10, Cell Signaling Technology), Vimentin (D21H3, Cell Signaling Technology), CD24 (ab199140 Abcam). Proteins were incubated with the primary antibodies over night at 4°C. They were then stained with anti-mouse, anti-rabbit or anti-goat secondary antibodies (Jackson Laboratory) for 60 minutes at room temperature. Thereafter they were incubated with chemiluminescent HRP substrate (WBKLS0500, Merck M) for 5 minutes. Chemiluminesence signals were collected via the Fujifilm LAS-3000 (Fuji, Japan) as per the manufacturer's instructions.

Immunocytochemistry and fluorescence assay

Cells were seeded onto 8-well culture slides (#354118, Falcon) overnight before fixation with 4% PFA for 10 minutes at room temperature followed by 1x PBS washes.

Cells were permeabilized with 0.5% Triton X-100/PBS for 5 minutes at room temperature, washed with 1x PBS, and blocked in 5% BSA (Sigma) in PBS for 60 minutes before incubating with Snail (20C8, ThermoFisher) primary antibodies followed by the secondary antibodies Alxea Fluor 594 (ThermoFisher). Slides were mounted in VECTASHIELD Mounting Medium with DAPI (H-1200; VECTOR Lab, Japan). Fluorescence images were visualized with Keyence fluorescence microscope.

Immunohistochemistry staining

Human gastric cancer tissue array (MLB Life Science Japan) and tumor specimens from mice gastric tumors were deparaffinized, rehydrated and placed in 3% (v/v) H_2O_2–methanol for 15 min at room temperature. The slides were then immersed in blocking solution (Non-specific Staining Blocking Reagent; Dako-Cytomation, Kyoto, Japan) for 15 min and incubated with the primary antibodies listed below at 4 ^{0}C overnight. Antigen–antibody complexes were detected with a secondary antibody (Histofine Simple Stain MAX PO (R) for rabbit monoclonal, or (G) for goat polyclonal (Nichirei, Tokyo, Japan) and visualized using 3,30-diaminobenzidine (0.5 mg/ml in Tris-buffered saline). The list of primary antibodies and dilution ratios were as follows: 1. Anti-SNAIL antibody (goat polyclonal, ab53519, Abcam), 1: 1,000; 2. Anti-CCN3 antibody (rabbit monoclonal, ab191425, Abcam), 1:100; 3. Anti-NEFL antibody (rabbit monoclonal, ab223343, Abcam), 1:400.

Flow cytometry

Incubation buffer was prepared as 1x PBS + 2% FBS. Single cell suspensions were washed with cooled incubation buffer, and re-suspended in 1x PBS + 2% FBS on ice for 30 minutes for antibody blocking: anti-CD24-FITC (ML5; Bio-legend, San Diego, CA), CD44-FITC (BJ18; Bio-legend, San Diego, CA) and DAPI (422801, Bio-legend, San Diego, CA). Cells were suspended in 0.5 mL incubation 1x PBS + 2% FBS to reach a final concentration of 10^6 cells/ml. Data were collected by the BD FACSCanto II or BD FACSVerse flow cytometer (Becton-Dickinson, Franklin Lakes, NJ) and analyzed with FlowJo software (TreeStar, San Carlos, CA). Cell debris was excluded from the analysis based on scatter signals, and fluorescent compensation was adjusted when double stained.

Statistical Analyses

Independent sample t tests were performed to compare the continuous variation of two groups, and the ~~χ^2 test or Fisher exact~~ student's test was applied for comparisons of variables. $P < 0.05$ was considered significant. All data are reported as mean ±SEM.

Results

Gastric Spheres Cultured Under Serum-Free Conditions Manifest Stem Cell Properties

Self-renewal capability is a major property of stem cells, and can be accurately assessed via sphere formation [15]. Gastric cancer cell lines produce stem-like sphere-forming cells when cultured under B-27 (+) bFGF (+) EGF (+) serum-free medium (CSC serum-free medium) in ultra-low attachment culture dishes [16]. The original gene expression profiles and tumor morphologies in cancer cells are well reflected in spheres cultured in the CSC serum-free condition [17]. We assessed the sphere-forming capacity of five gastric cancer cell lines for initial culture (cells were collected from attached condition and seeded in CSC serum-free medium) and passage culture (cells were collected from formed spheres and seeded in CSC serum-free medium), and found that three cell lines had the ability to form spheres (Figure 1A). Those spheres all originated from single cell and not by mere cell herds or aggregations, which was ensured by seeding single cells in 96 well plates and spheres managed to develop after several weeks (data not shown). Sphere-forming capacity of passaged cells (passage culture) was stronger compared with that of parental cells (initial culture), when the same number of cells were seeded in CSC serum-free medium (Figure 1B). To further confirm whether malignant cells possess additional stemness traits, 1 x 10^4 NCI-N87 cells were transplanted into the flanks of NOD/SCID mice. Histological analysis of xenografts exhibited an epithelial-like morphology irrespective of whether they were generated by parental or sphere cells (Figure 1C & S1);

however, sphere cells were more efficient at producing bulky tumors in NOD/SCID mice compared with parental monolayer cells (Figure 1D).

Gastric Spheres Express EMT-associated Factors

Acquisition of stemness traits in malignant cells is commonly achieved through undergoing EMT process, thus tracking the activities of EMT-associated factors will help uncovering mechanism behind the obtained stemness. Four key EMT factors were examined in this study, and higher mRNA expression of EMT factors (TWIST1, 2, SNAIL, and SLUG) were found in spheres compared with parental cells (Figure 2A). HGC27 cells, which form spheres most efficiently, highly expressed TWIST1 and SNAIL mRNAs compared with other two sphere-forming cell lines, NCI-N87 and NUGC3. Consistent with this, immunofluorescence images indicated highest protein expression of SNAIL in HGC27 cells (Figure 2B). The role of TWIST1 has been extensively investigated in previous EMT-associated researches [18]; therefore, HGC27 and SNAIL were chosen as the target cell line and molecule pair in the current study.

SNAIL Regulates Tumorigenicity in Gastric Cancer Cells

In order to investigate whether SNAIL regulates stemness and tumorigenicity in gastric spheres, we determined phenotypic alteration after lentivirus-mediated short-hairpin RNA-interfered knockdown of SNAIL (shRNA-SNAIL k.d.). Realtime quantitative PCR

indicated successful knockdown effects using shRNA-SNAIL in HGC27 cell li~~e~~nes and spheres (Figure 3A). Western blotting showed a similar tendency of 29 Da SNAIL protein expression (Figure 3B). Epithelial and mesenchymal traits of HGC27 were measured using antibodies against E-cadherin and Vimentin, representative proteins for epithelial and mesenchymal phenotypes, respectively. Up-regulation of E-cadherin with down-regulation of Vimentin by SNAIL knockdown indicated the event of mesenchymal-to-epithelial transition in HGC27 cell lines (Figure 3B). The most conspicuous phenomenon observed was that the shape of formed sphere in the CSC serum-free medium switched from having smooth margins into jagged and sharp edges by the SNAIL knockdown (Figure 3C). Previous studies reported a CD44+/CD24– subpopulation of gastric cancer contains gastric cancer stem cells [19]. As shown in Figure 3D, the fluorescence activated cell sorter analysis revealed that 91.0% of the HGC27 cell line was CD44+/CD24–, while knockdown of SNAIL in this cell line almost completely eliminates this population. This suggested that gastric cancer stem cells are maintained, at least in part, by the presence of SNAIL.

Stemness such as self-renewability in cancer cells is associated with the capacity of forming spheres out of the transformed epithelial cells [20]. Therefore, we compared sphere forming capacity between parental HGC27 and stabl~~y~~e SNAIL knockdown HGC27 cells cultured in monolayer conditions. The number and area of sphere were significantly decreased by SNAIL knockdown, suggesting a reduced ability to self-renewal (Figure 3E). Consistent with this, when 1 x 10^4 cells were transplanted into the flanks of NOD/SCID mice, although histological analysis did not show any significant alterations, stabl~~y~~e

SNAIL knockdown HGC27 cells were less efficient at producing bulky tumors ~~in~~ compared with parental HGC27 cells (Figure 3F).

Lower expression of SNAIL was referred to as increased sensitivity upon chemo-treatment due to diminished self-renewability in malignancy [21]. In our experimental condition, stabl~~y~~e SNAIL knockdown HGC27 cells were more susceptible to 5-fluorouracil (5-FU) treatment compared with parental HGC27 cells (Figure 3G).

Together, these findings SNAIL regulates tumorigenecity, possibly stemness at least in part, in gastric cancer cells.

SNAIL-regulating Genes in Gastric Cancer Cells

To unveil the mechanisms underlying phenotypic modifications induced by knockdown of SNAIL in HGC27 cells, gene expression microarray analysis on a HGC27-SNAIL knockdown and parental HGC27 cells was performed. Under the alteration of SNAIL expression, distributed genes movement were shown in Figure 4A. Of those genes, a total of 1656 and 1832 probe sets ($|FC| \geq 2$) were specifically upregulated or downregulated in stable HGC27-SNAIL knockdown cells, respectively (Figure 4B). Statistically overrepresented functional processes were obtained through enriched genes querying in the Gene Ontology (GO) database ($P < 0.05$; Figure 4C). The main processes enriched in up-/down-regulated genes include those pertaining to multiple binding and cellular processes. It is suggested that instead of individual activation, genes tend to

collaborate in genetic networks, thus we subjected the enriched GO processes that were selected as meaningful to REVIGO analysis, which is a useful web tool that summarizes long lists of GO terms. Several GO terms formed a treemap of the most significant processes: cell motility, chemotaxis, adhesion, neural regeneration, and cell death, as well as those involved in EMT (Figure 4D). Within this network, chemotaxis was a focal node and in the broader group of terms under the chemotaxis title, the regeneration process was chosen as a target to be studied in greater depth due to the possible role of neuron development and supervision in malignancy progression. ~~For example, Sox2 has been reported as the key regulator in CSCs and is over expressed in various tumors. Other significant genes included TGFB1 and NOTCH1; both belong to the Notch signaling pathway, which plays an important role in angiogenesis and CSC self-renewal [22]. Indeed, most of the significant GO terms identified are implicated in well-known signaling processes. Genes from this regeneration process were also included in EMT process with significant biological functions. Among them, Cellular Communication Network factor 3 (CCN3; also known as NOV or IGFBP9) as described in prostate cancer [23]. Meanwhile, Neurofilament Light Peptide (NEFL), was found to be expressed in a wide range of malignancies as a tumor suppressor gene [24].~~ qRT-PCR confirmed down- and up-regulation of CCN3 (also known as NOV or IGFBP9): Cellular Communication Network factor 3, and NEFL: Neurofilament Light peptide mRNA expression by SNAIL knockdown in HGC27cells (Figure 4E).

CCN3 and NEFL Expression in Gastric Cancers

The occurrence of distant metastases and poor survival outcome have been reported relevant with high SNAIL expression in gastric cancer patients [25]. CCN3 belongs to the CCN family (cysteine-rich protein 61 (CYR61)), connective tissue growth factor (CTGF), nephroblastoma overexpressed (NOV)). Limited information is known concerning the functional correlation between EMT with CCN3 and NEFL in cancers. There have been reports of increased expression of CCN3 in prostate and cervical cancers [23, 26]. CCN3 was demonstrated to promote EMT by activating the FAK/Akt/HIF-1α pathway in prostate cancer [27]. NEFL has been implicated in carcinogenesis as a putative suppressor gene in neuron related inhibition of both cell proliferation and invasion in head and neck squamous cell carcinoma [28]. Using data of transcript level of SNAIL, CCN3 and NEFL from The Cancer Genome Altas (TCGA) stomach adenocarcinoma project, each gene expression in gastric cancers and normal gastric tissues were shown in Figure 5A. There were no correlations in mRNA expression levels between SNAIL and either CCN3 or NEFL, and no correlation between CCN3 and NEFL (Figure 5B). Immunohistochemistry analysis was then performed on a paraffin-embedded human gastric cancer tissue array (n = 30, purchased from MBL Life Science, Japan). CCN3 expression was detected in 96.7% (29/30), NEFL expression was positive in 86.7% (26/30) and SNAIL expression occurred in 26.7% of tumor tissues (8/30). Representative staining with positive and negative images for Snail/CCN3/NEFL are shown in Figure 5C., ~~showing the direct expression distribution in human gastric cancer tissue.~~ Compared with Figure S2 of normal gastric tissues, CCN3

antibody only stained positive in some fibroblasts and myofibroblasts besides malignant parts; while NEFL also stained positive in neurofilament as reported elsewhere.

CCN3 and NEFL are Critical for SNAIL-Induced Stemness

We initially investigated how CCN3 and NEFL function by introducing their expression vectors into SNAIL knockdown HGC27 cells and parental HGC27 cells respectively, and those effects were confirmed with western blotting (Figure 6A). Forced expression of SNAIL or CCN3 in sh-SNAIL knockdown HGC27 cells resulted in significantly increased number of formed spheres (Figure 6B-a & b); while that of NEFL caused diminished sphere formation ability in parental HGC27 cells (Figure 6B-c). Furthermore, the chemoresistance against 5-FU of each pair of cells was also measured. The results were consistent with alterations to sphere formation capacity: the proliferation rates of HGC27-shSNAIL, HGC27-NEFL, and HGC27-shSNAIL-CCN3 cells were reduced more rapidly when 5-FU was added in a dose-dependent manner (Figure 6C). The fact that HGC27-shSNAIL stable knockdown cells produced significantly reduced tumor masses compared with SNAIL re-introduced rescue cells was proved via xenograft assays in vivo (data not shown). To further evaluate the role of NEFL molecule during EMT process, gastric cancer cell line IM95 was selected from several candidate cell lines due to high NEFL expression level. Several observations can be witnessed after knockdown of NEFL in IM95: steady knockdown of NEFL using shRNA in IM95 cell was established and verified (Figure 6D-a & b), with enhanced mesenchymal and decreased epithelial

indexes of vimentin and E-cadherin discovered from knockdown of NEFL respectively (Figure 6D-b), and increased chemo-resistance effect throughout proliferation assay with 5FU addition as well (Figure 6D-c).

Discussion

In this study, we established three spheres enriched in CD44+ gastric cancer cells. The spheres displayed EMT phenotype, high tumorigenecity, and chemoresistance against 5-FU treatment. SNAIL, one of the key regulators of EMT, was upregulated in the spheres, and CCL3 and NEFL were further extracted as downstream targets of SNAIL by microarray analyses. Re-introduction of CCN3 and NEFL partially rescued and impaired the SNAIL-dependent CSC like activity, tumorigenicity, and chemoresistance in HGC-27 gastric cancer cells, respectively.

Previous studies have uncovered that CD44, EPCAM, CD133, CD24, CD166 or Aldh are CSC markers in certain circumstances and are enriched in spheres generated from gastric cancer cell lines or clinical tissues [29, 30]. Although it stills opens to be discussed whether all CD44+ cells are CSCs, the CD44+ subpopulation is reported to prevail in cancer cells after spheres are formed. In this study, we also showed that the CD44+ subpopulation was enriched in gastric spheres.

In a mammospheres formation assay, expression of EMT-associated factors, such as TWIST1/2, SNAIL, and SLUG in breast cancer cells are up-regulated and associated with the acquisition of CSC propert~~y~~ies and greater metastatic ability after EMT process [31]. These EMT-associated molecules are involved in multiple signaling pathways in other types of cancers. In the present study, expression of TWIST1 and SNAIL were significantly elevated in gastric spheres, especially in HGC27-derived spheres. The role of TWIST1 in EMT processes during gastric carcinogenesis has been extensively investigated [32, 33],

while that of SNAIL has not been researched as much as TWIST1~~remains obscure~~. Therefore, we focused on the functional analyses of SNAIL and its downstream targets in gastric carcinogenesis. Indeed, we showed that knockdown of SNAIL resulted in acquisition of EMT-phenotype and loss of CD44+ cell population. It also led to the impaired growth of gastric cancer xenografts and chemoresistance against 5-FU treatment. These data are consistent with discoveries reported in other solid malignancies [34-36], and indicates crucial roles of SNAIL in regulating CSC properties.

To further explore the underlying mechanisms of SNAIL-mediated gastric carcinogenesis, we performed microarray analyses which revealed transcriptome alterations by knockdown of SNAIL. GO terms formed a treemap of the most significant processes: cell motility, chemotaxis, adhesion, neural regeneration, and cell death, as well as those involved in EMT. Among the components from the network of chemotaxis, ~~F~~for example, Sox2 has been reported as the key regulator in CSCs and is over expressed in various tumors. Other significant genes included TGFB1 and NOTCH1; both belong to the Notch signaling pathway, which plays an important role in angiogenesis and CSC self-renewal [22]. Indeed, most of the significant GO terms identified are implicated in well-known signaling processes. Genes from this regeneration process were also included in EMT process with significant biological functions. Among them, ~~Cellular Communication Network factor 3 (~~CCN3~~; also known as NOV or IGFBP9)~~ as is described in prostate cancer [23]. Meanwhile, ~~—~~ ~~Neurofilament Light Peptide (~~NEFL~~)~~, was found to be expressed in a wide range of malignancies as a tumor suppressor gene [24]. Based on study interest,

CCN3 and NEFL were here chosen as two possible downstream targets of SNAIL that seem to function in stemness in gastric cancer.

CCN3 belongs to the three-member family of cysteine-rich regulatory proteins and has been found in various cancer cells and surrounding tissues, suggesting that in the cancer microenvironment, it is likely that CCN3 may act as a EMT-regulatory factor [37]. Consistent with this, CCN3 requires its C-terminal domain for bone metastatic function, and is correlated with aggressive disease progression in prostate cancer [38]. In hepatocellular carcinoma, after being secreted from hepatic cells, CCN3 gained its' activity in various processes during EMT via HSCs (Hepatic stellate cells) [39]. A previous study has also shown that increased expression level of CCN3 expression lead to local invasion and distant metastases in gastric cancer [40, 44]. In this study, we showed a link between CCN3 expression and gastric stemness properties, and have further shown that low levels of CCN3 in HGC27 cells result in reduced stemness and tumorigenicity. Therefore, approaches capable of reducing CCN3 expression may have the potential to suppress EMT and to be novel therapies against gastric cancer.

NEFL, which practically maintains the neuronal caliber and functions as a regulator in intracellular transport to axons and dendrites, has also be implicated in various carcinogenesis [41]. NEFL acts as a tumor suppressor in non-small cell lung cancer (NSCLC), inhibiting invasion and metastasis, while methylation may destroy its protective effect [42]. In NSCLC and breast cancer, patients with higher expression of NEFL mRNA transcript had a better five-year disease-free survival [24]. In contrast to these reports, our

study showed that NEFL might enhance the tumor development in xenografts. The reason behind the contrasting outcomes may be due to the fact that in the advanced stage of malignancy, cancer cells tend to become much fiercer in metastatic potential and phenotypes, thus the invasions are nowhere to be hold arrested by merely cytoprotective genes expression alterations [43]. In either case, NEFL in digestive system cancers such as gastric cancer may play distinct roles in a context-dependent manner.

In conclusion, we showed that SNAIL regulates the expression of CCN3 and NEFL genes in human gastric cancer cells, and that these in turn control the CSC activities. Strategies that disrupt this possible circle may be possible to treat gastric cancer in future. Double antagonists targeting both CCN3/NEFL-SNAIL axis may weaken the malignant progression and dual RNAi study should be considered before RNAi compound development. Also, protein secretion of the target molecule that plays important roles in malignancy can be traced and intentionally attacked through clonal antibody. Multiple channels of further application as therapeutic agents may be helpful for patients with gastric cancer.

Competing Interests:

We have received research funds under contract from Sumitomo Danippon Pharma Co., Ltd.

References:

1. Rawla P, Barsouk A.Epidemiology of gastric cancer: global trends, risk factors and prevention. Prz Gastroenterol. 2019; 14: 26–38.

2. Afify SM, Seno M. Conversion of stem cells to cancer stem cells: undercurrent of cancer initiation. Cancers (Basel). 2019; 11: 345.

3. Jolly MK, Celià-Terrassa TDynamics of phenotypic heterogeneity associated with EMT and stemness during cancer progression. J. Clin. Med. 2019, 8, 1542.

4. Hollier BG, Tinnirello AA, Werden SJ, Evans KW, Taube JH, Sarkar TR, et al. Tinnirello, FOXC2 expression links epithelial-mesenchymal transition and stem cell properties in breast cancer. Cancer Res. 2013; 73: 1981–1992.

5. Mani SA, Guo W, Liao MJ, Eaton EN, Ayyanan A, Zhou AY,et al. The epithelial-mesenchymal transition generates cells with properties of stem cells. Cell. 2008; 133: 704–715.

6. Guen VJ, Chavarria TE, Kröger C, Ye X, Weinberg RA, Lees JA. EMT programs promote basal mammary stem cell and tumor-initiating cell stemness by inducing primary ciliogenesis and Hedgehog signaling. PNAS. 2017; 114: E10532–E10539.7. Wang Y, Shi J, Chai K, Ying X, P Zhou B. The role of snail in EMT and tumorigenesis. Curr Cancer Drug Targets. 2013; 13: 963–972.

7. Cristina Peña, José Miguel García, Javier Silva, Vanesa García, Rufo Rodríguez, Isabel Alonso, et al. E-cadherin and vitamin D receptor regulation by SNAIL and ZEB1 in colon cancer: clinicopathological correlations. Human Molecular Genetics. 2005; 14: 3361–3370.

8. Brzozowa M, Michalski M, Wyrobiec G, Piecuch A, Dittfeld A, Harabin-Słowińska M, et al. The role of Snail1 transcription factor in colorectal cancer progression and metastasis. Contemp Oncol (Pozn). 2015; 19: 265–270.

9. Serrano-Gomez SJ, Maziveyi M, Alahari SK. Regulation of epithelial-mesenchymal transition through epigenetic and post-translational modifications. Mol Cancer. 2016; 15: 18.

10. Tusher VG, Tibshirani R, Chu G.Significance analysis of microarrays applied to the ionizing radiation response.Proc Natl Acad Sci USA. 2001; 98 (9): 5116–5121.

11. Gautier L, Cope L, Bolstad BM, Irizarry RA. affy—analysis of Affymetrix GeneChip data at the probe level. Bioinformatics. 2004 12; 20: 307–315.25. Huang DW, Sherman BT, Lempicki RA.Systematic and integrative analysis of large gene lists using DAVID Bioinformatics Resources. Nature Protoc. 2009; 4: 44–57.

12. Walter, Wencke, Fatima Sanchez-Cabo, and Mercedes Ricote. GOplot: an R package for visually combining expression data with functional analysis. Bioinformatics. 2015; 31: 2912-2914.

13. Fran Supek ,Matko Bošnjak,Nives Škunca,Tomislav Šmuc. REVIGO Summarizes and Visualizes Long Lists of Gene Ontology Terms. PLoS ONE. 2011 July 18.

14. Huang DW, Sherman BT, Lempicki RA. Bioinformatics enrichment tools: paths toward the comprehensive functional analysis of large gene lists. Nucleic Acids Res. 2009; 37: 1–13.

15. Al-Hajj M, Clarke MF. Self-renewal and solid tumor stem cells. Oncogene. 2004; 23: 7274–82.28. Ni SJ, Zhao LQ, Wang XF, Wu ZH, Hua RX, Wan CH, et al. CBX7 regulates stem cell-like properties of gastric cancer cells via p16 and AKT-NF-κB-miR-21 pathways. J Hematol Oncol. 2018; 11: 17.

16. Seon Ok Min, Sang Woo Lee, Seon Young Bak, Kyung Sik Kim. Ideal sphere-forming culture conditions to maintain pluripotency in a hepatocellular carcinoma cell lines. Cancer Cell Int. 2015; 15:95.

17. Ishiguro T, Ohata H, Sato A, Yamawaki K, Enomoto T, Okamoto K. Tumor-derived spheroids: Relevance to cancer stem cells and clinical applications. Cancer Sci. 2017; 108: 283–289.

18. Chang Ohk Sung, Keun-Woo Lee, Songying Han, and Seok-Hyung Kim. Twist1 Is Up-Regulated in Gastric Cancer-Associated Fibroblasts with Poor Clinical Outcomes. Am J Pathol. 2011; 179: 1827–1838.

19. Takaishi S, Okumura T, Tu S, Wang SS, Shibata W, Vigneshwaran R, et al. Identification of gastric cancer stem cells using the cell surface marker CD44. Stem Cells. 2009; 27: 1006–1020.

20. Lim S, Becker A, Zimmer A, Lu J, Buettner R, Kirfel J. SNAI1-mediated epithelial-mesenchymal transition confers chemoresistance and cellular plasticity by regulating genes involved in cell death and stem cell maintenance. PLoS ONE. 2013; 8.

21. Smith, Bethany N, and Valerie A Odero-Marah. The role of Snail in prostate cancer. Cell adhesion & migration. 2012; 6: 433-41.

22. Venkatesh V, Nataraj R, Thangaraj GS, Karthikeyan M, Gnanasekaran A, et al. Targeting Notch signaling pathway of cancer stem cells. Stem Cell Investig. 2018; 5: 5.

23. Maillard M, Cadot B, Ball RY, Sethia K, Edwards DR, Perbal B, et al. Differential expression of the ccn3 (nov) proto-oncogene in human prostate cell lines and tissues. Mol Pathol. 2001; 54: 275–280.

24. Li XQ, Li L, Xiao CH, Feng YM. NEFL mRNA Expression Level Is a Prognostic Factor for Early-Stage Breast Cancer Patients. PLOS One. 2012; 7: e31146.

25. Klaudia Skrzypek, Marcin Majka. Interplay among SNAIL Transcription Factor, MicroRNAs, Long Non-Coding RNAs, and Circular RNAs in the Regulation of Tumor Growth and Metastasis. Cancers. 2020; 12:1.

26. Zhang T, Zhao C, Luo L, Xiang J, Sun Q, Cheng J, et al. The clinical and prognostic significance of CCN3 expression in patients with cervical cancer. Adv Clin Exp Med. 2013; 22: 839–45.

27. Chen PC, Tai HC, Lin TH, Wang SW, Lin CY, Chao CC, et al. CCN3 promotes epithelial-mesenchymal transition in prostate cancer via FAK/Akt/HIF-1α-induced twist expression. Oncotarget. 2017; 8: 74506–74518.

28. Huang Z, Zhuo Y, Shen Z, Wang Y, Wang L, Li H, et al. The role of NEFL in cell growth and invasion in head and neck squamous cell carcinoma cell lines. J Oral Pathol Med. 2014; 43:191–198.

29. Phu Hung Nguyen, Julie Giraud, Lucie Chambonnier, Pierre Dubus, Linda Wittkop, Geneviève Belleannée, et al. Characterization of Biomarkers of Tumorigenic and Chemoresistant Cancer Stem Cells in Human Gastric Carcinoma. Clin Cancer Res. 2017; 23: 6.

30. Xiao-Long Chen, Xin-Zu Chen, Yi-Gao Wang, Du He, Zheng-Hao Lu, Kai Liu, et al. Clinical significance of putative markers of cancer stem cells in gastric cancer: A retrospective cohort study. Oncotarget. 2016; 7: 38.

31. I. K. Guttilla, K. N. Phoenix, X. Hong, J. S. Tirnauer, K. P. Claffey, B. A. White. Prolonged mammosphere culture of MCF-7 cells induces an EMT and repression of the estrogen receptor by microRNAs. Breast Cancer Res Treat. 2012; 132:75–85.

32. Jianxin Qian, Yizhou Luo, Xiaoqiang Gu, Wang Zhan, and Xi Wang. Twist1 Promotes Gastric Cancer Cell Proliferation through Up-Regulation of FoxM1. PLoS One. 2013; 8: e77625.

33. Rosivatz E, Becker I, Specht K, Fricke E, Luber B, Busch R, Höfler H, Becker KF. Differential expression of the epithelial-mesenchymal transition regulators snail, SIP1, and twist in gastric cancer. Am J Pathol. 2002; 161: 1881-91.

34. Arti Yadav, Bhavna Kumar, Jharna Datta, Theodoros N. Teknos, and Pawan Kumar. IL-6 promotes head and neck tumor metastasis by inducing epithelial-mesenchymal transition via the JAK-STAT3-SNAIL signaling pathway. Mol Cancer Res; 2011; 9.

35. Cornelia Kröger, Alexander Afeyan, Jasmin Mraz, Elinor Ng Eaton, Ferenc Reinhardt, et al. Acquisition of a hybrid E/M state is essential for tumorigenicity of basal breast cancer cells. PNAS. 2019; 116: 7353-7362.

36. Osorio, L. A., Farfán, N. M., Castellón, E. A., Contreras, H. R. SNAIL transcription factor increases the motility and invasive capacity of prostate cancer cells. Molecular Medicine Reports. 2016; 13: 778-786.

37. Kim H, Son S, Shin I. Role of the CCN protein family in cancer. BMB Rep. 2018; 51: 486–492.

38. Dankner M, Ouellet V, Desreumaux-Communal L, Schmitt E, Perkins D, Annis MG, et al. CCN3 is a prognostic biomarker and functional mediator of prostate cancer bone metastasis. AACR; Cancer Res 2019;79.

39. Li W, Liao X, Ning P, Cao Y, Zhang M, Bu Y, et al. Paracrine effects of CCN3 from non-cancerous hepatic cells increase signaling and progression of hepatocellular carcinoma. BMC Cancer. 2019; 19: 395.

40. Li J, Gao X, Ji K, Sanders AJ, Zhang Z, Jiang WG, et al. Differential expression of CCN family members CYR611, CTGF and NOV in gastric cancer and their association with disease progression. Oncol Rep. 2016; 36: 2517–2525.

41. Yuan A, Rao MV, Veeranna, Nixon RA. Neurofilaments at a glance. J Cell Sci. 2012;125: 3257–3263.

42. Shen Z, Chen B, Gan X, Hu W, Zhong G, Li H, et al. Methylation of neurofilament light polypeptide promoter is associated with cell invasion and metastasis in NSCLC. Biochem Biophys Res Commun. 2016; 470: 627-634.

43. Yokota J. Tumor progression and metastasis. Carcinogenesis. 2000; 21: 497-503.

44. Tsu-Yao Cheng, Ming-Shiang Wu, Kuo-Tai Hua, Min-Liang Kuo, Ming-Tsan Lin, et al. Cyr61/CTGF/Nov family proteins in gastric carcinogenesis. World J Gastroenterol. 2014; 20: 1694-1700.

Legends:

Figure 1. Characteristics of gastric cancer cell lines spheres cultured under serum-free condition.

A. Photographic pictures of sphere morphology.

Initial and passage sphere assay were shown in upper and lower lane pattern respectively with each cell line marked on top.

B. Sphere formed per $2x10^4$ seeded cells as an index of cell renewal capacity.

a: sphere count; b: volume summary of sphere formed. Results were expressed as mean ± SD, * $p<0.05$; ** $p<0.01$.

C. Enhanced in vivo tumor volume formed from spheres in mice at an injection concentration of 4×10^4 cells.

D. Representative H&E slides from gastric cancer cell line NCI-N87 with their sphere formed tumors. Scale bar=200μm.

Figure 2. Stem cell properties and tumor malignancy in gastric cancer spheres.

A. Comparison of EMT factors on absolute mRNA expression levels in gastric cancer cell lines.

B. Immunofluorescence of SNAIL expression in HGC27, IM95 and FU97 cell lines.

a. Cells in the gastric cancer cell lines ~~HGC27~~ were found to express SNAIL (imaged with red fluorescent) in the nuclei;

b. Image with DAPI to identify the nuclei of ~~HGC27~~gastric cancer cells;

c. Merged image superimposed on a differential interference contrast background confirms co-localization. Scale bar=50μm.

Figure 3. SNAIL is sufficient and essential for induction of self-renewal and malignancy in gastric cancer cell line HGC27. (Knockdown is represented as k.d.).

A. Real-time quantitative PCR validation of SNAIL expression level in HGC27 and its stable SNAIL knockdown cell lines.

B. Effects of SNAIL knockdown on the expression of E-cadherin and Vimentin in HGC27 cell line.

C. Morphology alteration of gastric cancer cell line HGC27 after SNAIL knockdown in ultra-low attachment condition.

D. CD24 and CD44 FACS profiles of HGC27 and HGC27 SNAIL knockdown cell lines.

E. Sphere formed per $2x10^4$ seeded cells from HGC27 and HGC27 SNAIL knockdown cell.

F. Diminished in vivo tumorigenicity formed from HGC27 SNAIL knockdown cells in NOD/SCID mice at an injection concentration of $4x10^4$ cells. H&E staining of representative tumors, scale bar=200μm.

G. Decreased chemoresistance of HGC27 SNAIL knockdown cells compared with HGC27 when treated with 5-FU.

Figure 4. Microarray analysis between HGC27 and its SNAIL knockdown samples.

A. Plot analysis of distribution visualization of differentially expressed genes comparing SNAIL knockdown and control groups.

B. Bar plot detailing presented numbers of genes under SNAIL up/down regulation in two conditions.

C. GO terms enrichment analysis of molecular function, cellular component and biological process of differentially expressed genes (left to right).

D. The KEGG enrichment analysis of differentially expressed genes.

E. Real-time quantitative PCR validation of CCN3 and NEFL expression level in HGC27 and its stable SNAIL knockdown cell lines.

Figure 5. Elevated expression of SNAIL and CCN3 in patients with stomach adenocarcinoma.

A. mRNA transcript expression levels of SNAIL (a), CCN3 (b) and NEFL (c) are elevated in patients with gastric cancer from TCGA-STAD database. Box in red: malignant tissue; box in gray: normal tissue. ~~* p<0.05.~~

B. No correlation existed between CCN3 and NEFL in gastric cancer patients from TCGA-STAD database.

C. SNAIL, CCN3 and NEFL are highly expressed in human gastric cancer tissues.

Representative immunohistochemical staining (IHC) images of SNAIL, CCN3 and NEFL in gastric cancer tissues. Scale bar = 50 μm.

Figure 6. CCN3 and NEFL correlate with self-renewal and chemoresistance traits in gastric cancer cells.

A. Western blotting analysis of NEFL and CCN3 expression in associated cell lines.

B. Sphere formed per $2x10^4$ seeded cells as an index of cell renewal capacity.

a. HGC27 SNAIL knockdown vs. HGC27 SNAIL knockdown with SNAIL re-introduction;

b. HGC27 vs. HGC27 with NEFL introduction;

c. HGC27 SNAIL knockdown vs. HGC27 SNAIL knockdown with CCN3 re-introduction.

C. Chemoresistance alteration of SNAIL (a), CCN3 (b) and NEFL (c) introduction into associated HGC27 cell lines when treated with 5-FU. Results are expressed as mean ± SD, * $p<0.05$; ** $p<0.01$.

D. Knockdown of NEFL promoted the mesenchymal traits in gastric cancer cell line IM95.

a. Real time qPCR validation of NEFL expression level in IM95 and its stable NEFL knockdown cell lines.

b. Effects of NEFL knockdown on the expression of E-cadherin and Vimentin in IM95 cell line.

c. Increased chemoresistance of IM95 NEFL knockdown cells compared with IM95 cells when treated with 5-FU. Results are expressed as mean ± SD, * $p<0.05$; ** $p<0.01$.

Figure S1. Enhanced in vivo tumor volume formed from spheres in mice at an injection concentration of 4 x 10^4 cells of HGC27 and NUGC3 cells. Representative H&E slides from gastric cancer cell lines with their sphere formed tumors. Scale bar=200μm.

Figure S2. Representative immunohistochemical staining (IHC) images of CCN3 and NEFL in gastric normal tissues. Scale bar = 50 μm.

Table S1. Primer sequences

GAPDH	forward	5' -GAC ATC AAG AAG GTG GTG AAG C- 3'
	reverse	5' -GTC CAC CAC CCT GTT GCT GTA G- 3'
TWIST1	forward	5' -CTC AGC AGG GCC GGA GAC CT- 3'
	reverse	5' -CCC CAC GCC CTG TTT CTT TGA- 3'
TWIST2	forward	5' -CTC AGC AGG GCC GGA GAC CT- 3'
	reverse	5' -CCC CAC GCC CTG TTT CTT TGA- 3'
SNAIL	forward	5' -TCT CTA GGC CCT GGC TGC TAC A- 3'
	reverse	5' -CGC CTG GCA CTG GTA CTT CTT G- 3'
SLUG	forward	5' -GAA GAT GCA TAT TCG GAC CCA CAC- 3'
	reverse	5' -TTG ACC TGT CTG CAA ATG CTC TGT- 3'

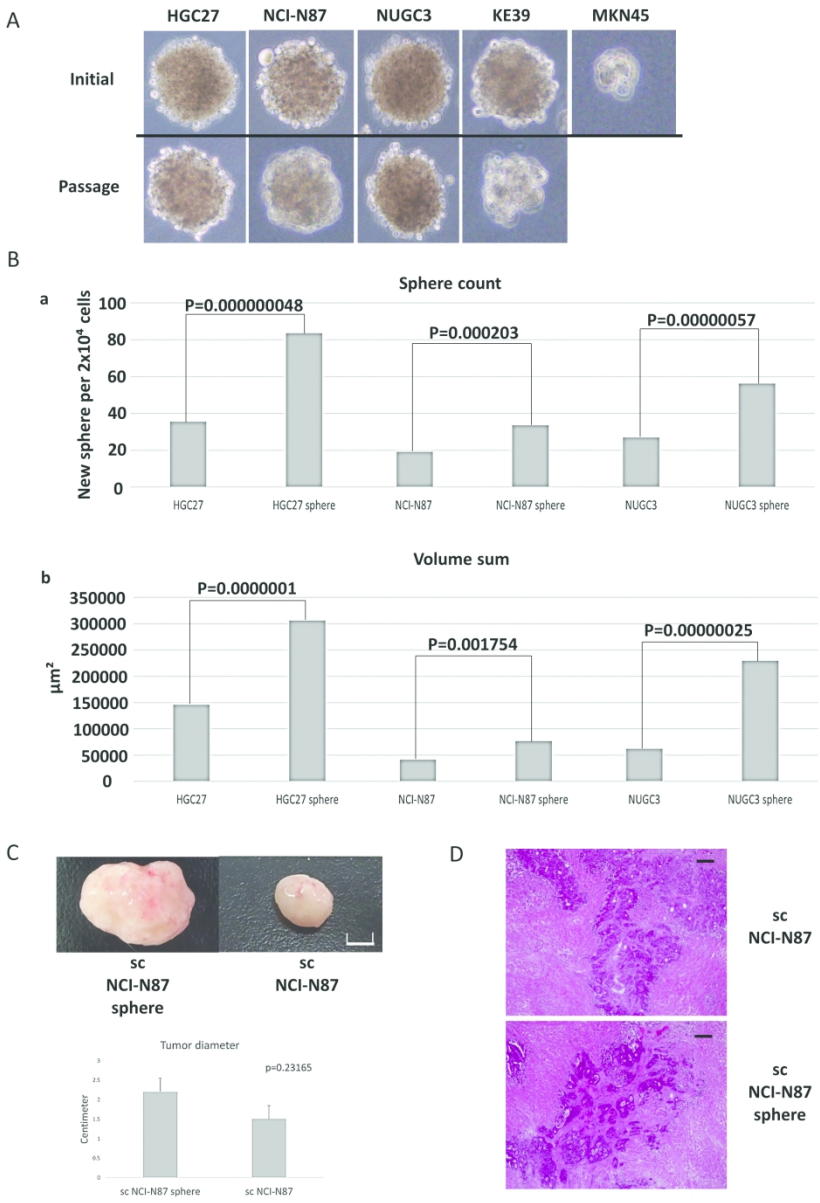

Characteristics of gastric cancer cell lines spheres cultured under serum-free condition.A. Photographic pictures of sphere morphology. Initial and passage sphere assay were shown in upper and lower lane pattern respectively with each cell line marked on top. B. Sphere formed per $2x10^4$ seeded cells as an index of cell renewal capacity.a: sphere count; b: volume summary of sphere formed. Results were expressed as mean ± SD, * $p<0.05$; ** $p<0.01$.C. Enhanced in vivo tumor volume formed from spheres in mice at an injection concentration of 4×10^4 cells.D. Representative H&E slides from gastric cancer cell line NCI-N87 with their sphere formed tumors. Scale bar=200µm.

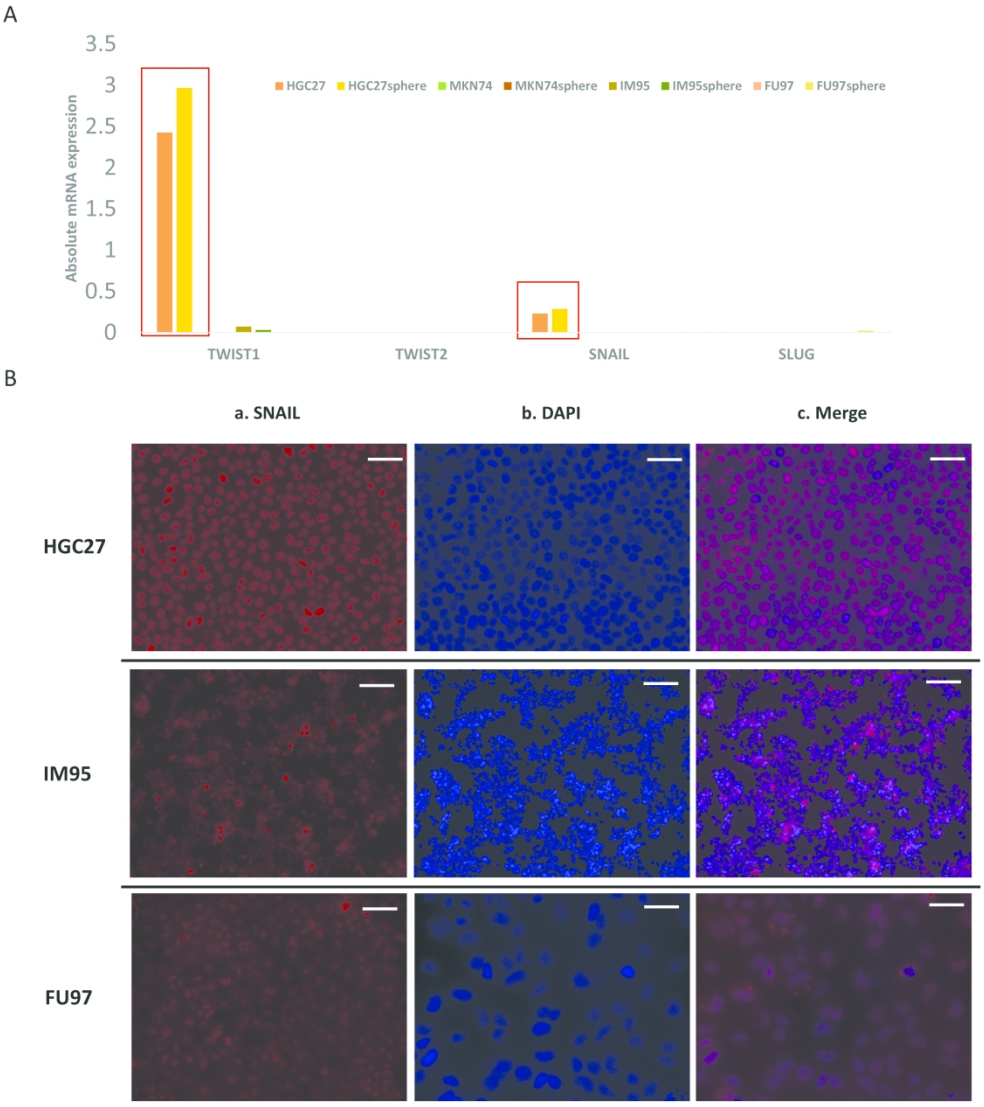

Stem cell properties and tumor malignancy in gastric cancer spheres.
A. Comparison of EMT factors on absolute mRNA expression levels in gastric cancer cell lines.
B. Immunofluorescence of SNAIL expression in HGC27, IM95 and FU97 cell lines.
a. Cells in the gastric cancer cell lines were found to express SNAIL (imaged with red fluorescent) in the nuclei;
b. Image with DAPI to identify the nuclei of gastric cancer cells;
c. Merged image superimposed on a differential interference contrast background confirms co-localization.
Scale bar=50μm.

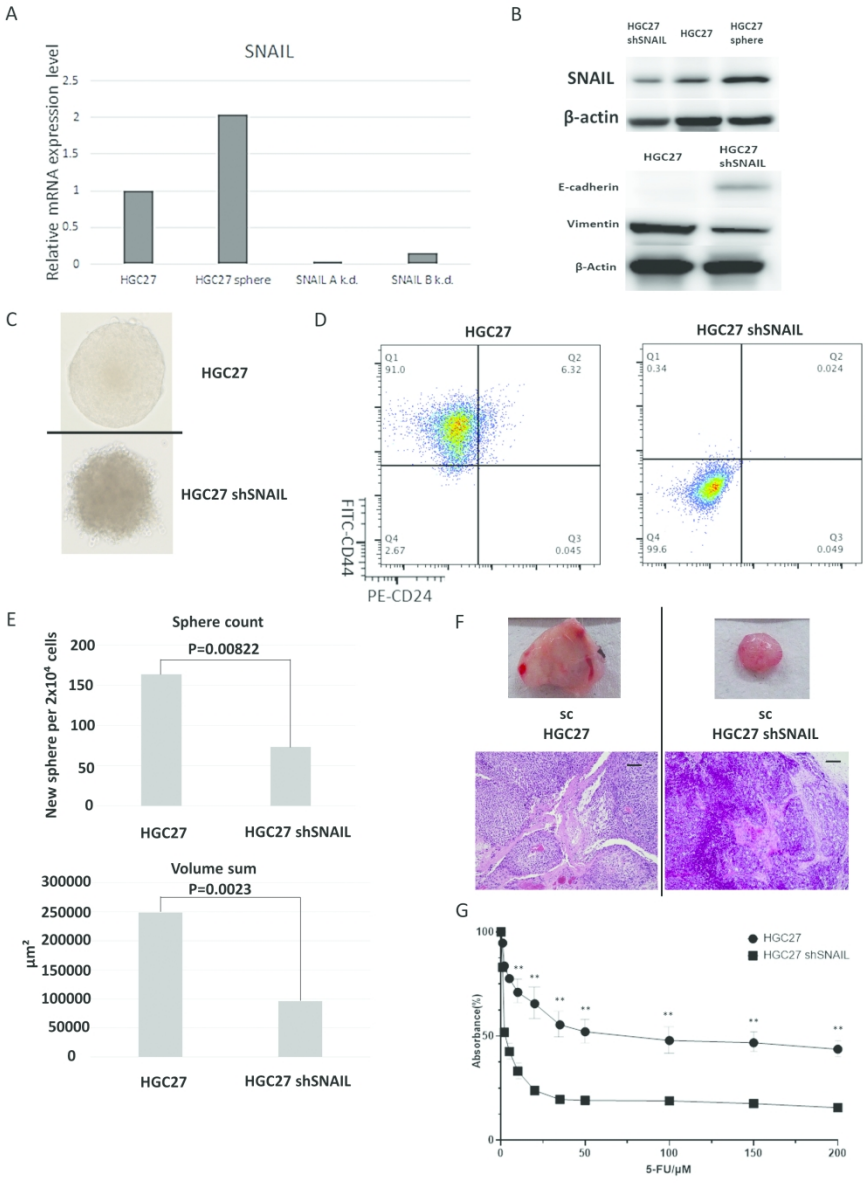

SNAIL is sufficient and essential for induction of self-renewal and malignancy in gastric cancer cell line HGC27. (Knockdown is represented as k.d.).A. Real-time quantitative PCR validation of SNAIL expression level in HGC27 and its stable SNAIL knockdown cell lines.B. Effects of SNAIL knockdown on the expression of E-cadherin and Vimentin in HGC27 cell line. C. Morphology alteration of gastric cancer cell line HGC27 after SNAIL knockdown in ultra-low attachment condition. D. CD24 and CD44 FACS profiles of HGC27 and HGC27 SNAIL knockdown cell lines.E. Sphere formed per $2x10^4$ seeded cells from HGC27 and HGC27 SNAIL knockdown cell.F. Diminished in vivo tumorigenicity formed from HGC27 SNAIL knockdown cells in NOD/SCID mice at an injection concentration of $4x10^4$ cells. H&E staining of representative tumors, scale bar=200μm.G. Decreased chemoresistance of HGC27 SNAIL knockdown cells compared with HGC27 when treated with 5-FU.

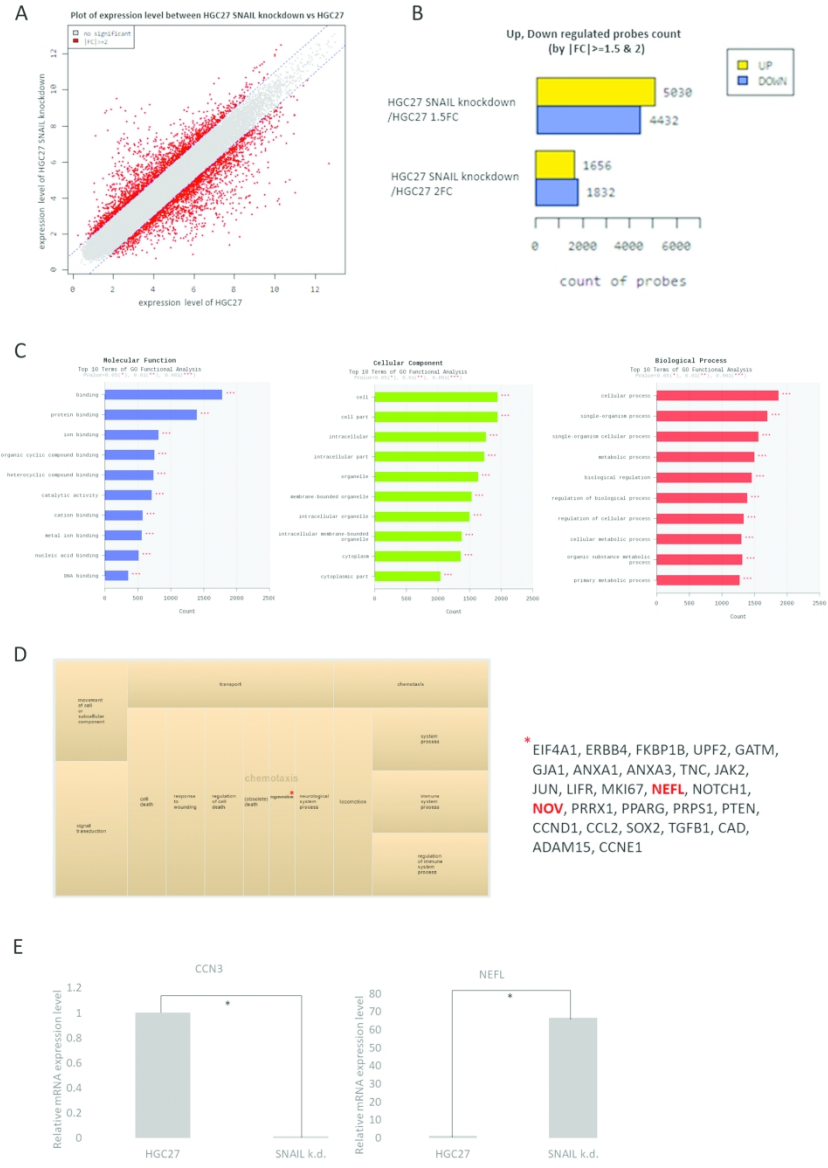

Microarray analysis between HGC27 and its SNAIL knockdown samples.
A. Plot analysis of distribution visualization of differentially expressed genes comparing SNAIL knockdown and control groups.
B. Bar plot detailing presented numbers of genes under SNAIL up/down regulation in two conditions.
C. GO terms enrichment analysis of molecular function, cellular component and biological process of differentially expressed genes (left to right).
D. The KEGG enrichment analysis of differentially expressed genes.
E. Real-time quantitative PCR validation of CCN3 and NEFL expression level in HGC27 and its stable SNAIL knockdown cell lines.

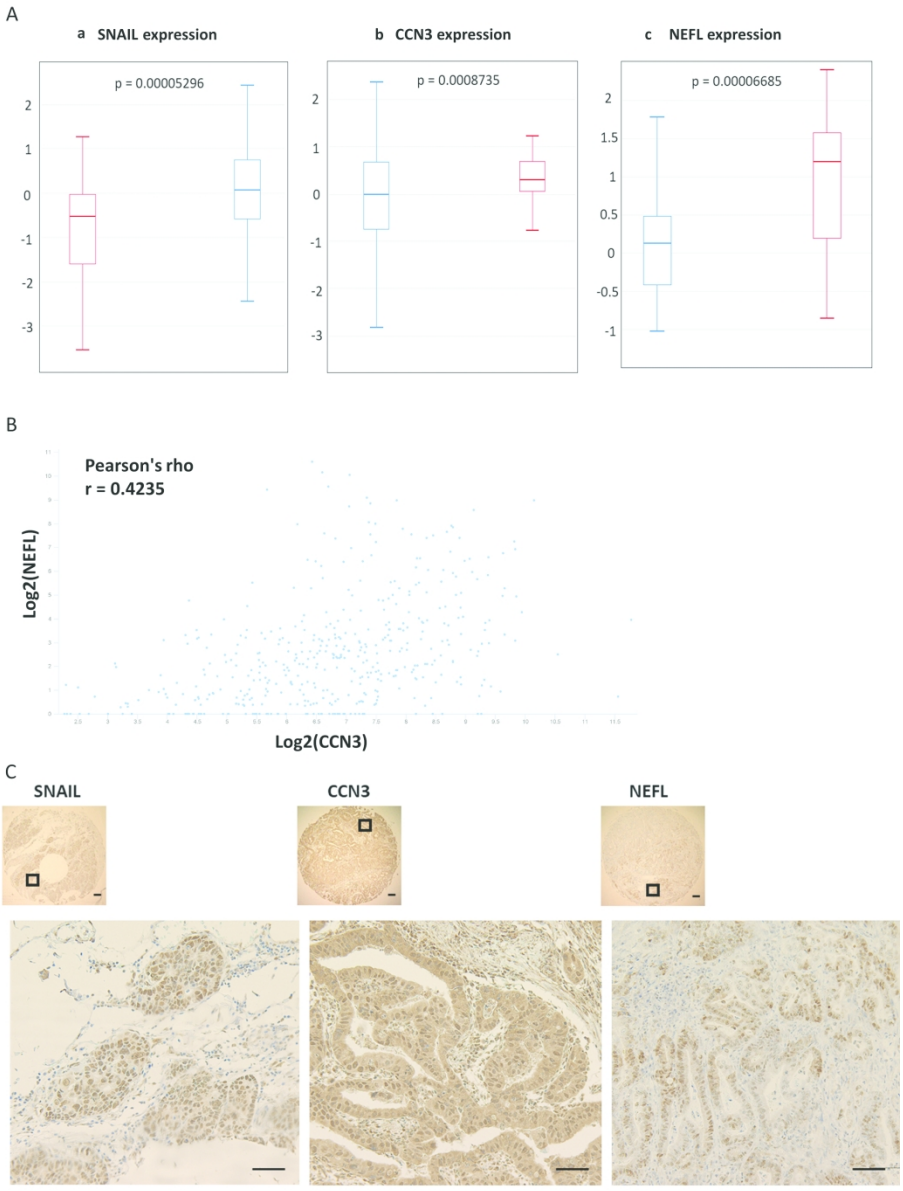

Elevated expression of SNAIL and CCN3 in patients with stomach adenocarcinoma.A. mRNA transcript expression levels of SNAIL (a), CCN3 (b) and NEFL (c) are elevated in patients with gastric cancer from TCGA-STAD database. Box in red: malignant tissue; box in blue: normal tissue.B. No correlation existed between CCN3 and NEFL in gastric cancer patients from TCGA-STAD database.C. SNAIL, CCN3 and NEFL are highly expressed in human gastric cancer tissues.Representative immunohistochemical staining (IHC) images of SNAIL, CCN3 and NEFL in gastric cancer tissues. Scale bar = 50 μm.

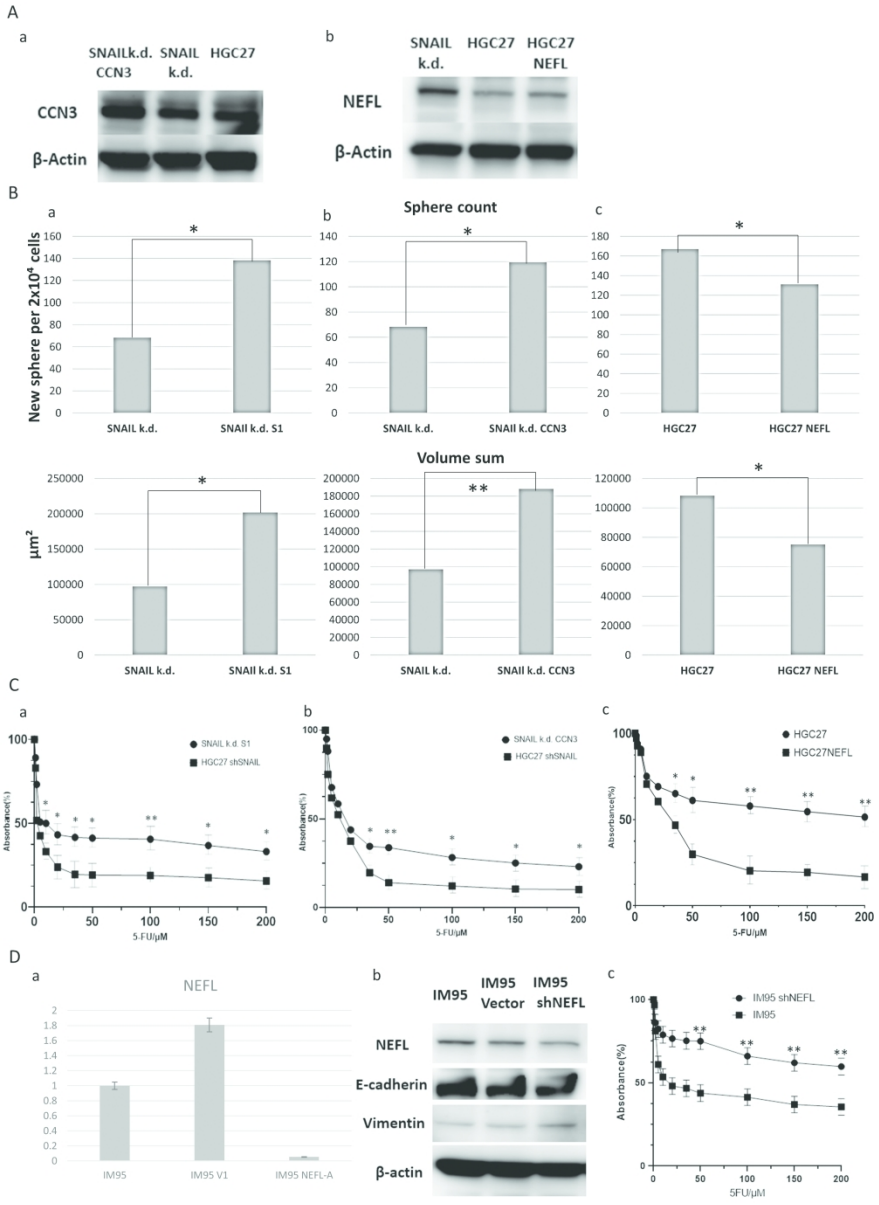

CCN3 and NEFL correlate with self-renewal and chemoresistance traits in gastric cancer cells.
A. Western blotting analysis of NEFL and CCN3 expression in associated cell lines.
B. Sphere formed per 2x10⁴ seeded cells as an index of cell renewal capacity.
a. HGC27 SNAIL knockdown vs. HGC27 SNAIL knockdown with SNAIL re-introduction;
b. HGC27 vs. HGC27 with NEFL introduction;
c. HGC27 SNAIL knockdown vs. HGC27 SNAIL knockdown with CCN3 re-introduction.
C. Chemoresistance alteration of SNAIL (a), CCN3 (b) and NEFL (c) introduction into associated HGC27 cell lines when treated with 5-FU. Results are expressed as mean ± SD, * $p<0.05$; ** $p<0.01$.
D. Knockdown of NEFL promoted the mesenchymal traits in gastric cancer cell line IM95.
a. Real time qPCR validation of NEFL expression level in IM95 and its stable NEFL knockdown cell lines.
b. Effects of NEFL knockdown on the expression of E-cadherin and Vimentin in IM95 cell line.
c. Increased chemoresistance of IM95 NEFL knockdown cells compared with IM95 cells when treated with 5-FU. Results are expressed as mean ± SD, * $p<0.05$; ** $p<0.01$.

Figure S1

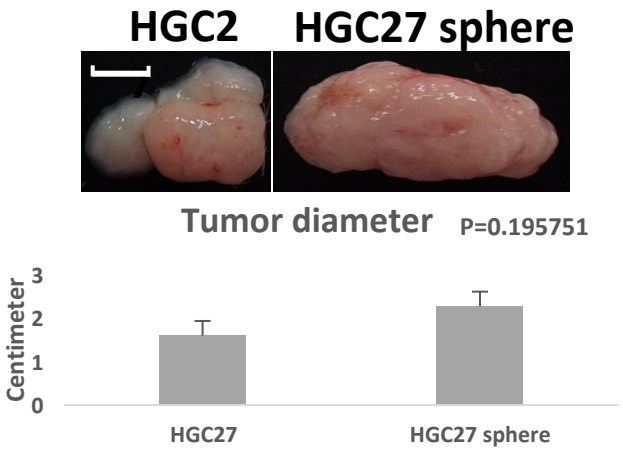

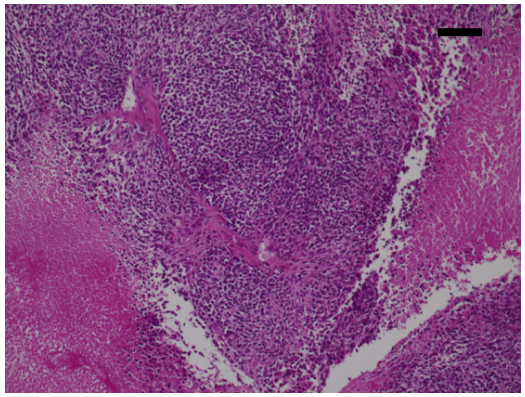

sc HGC27

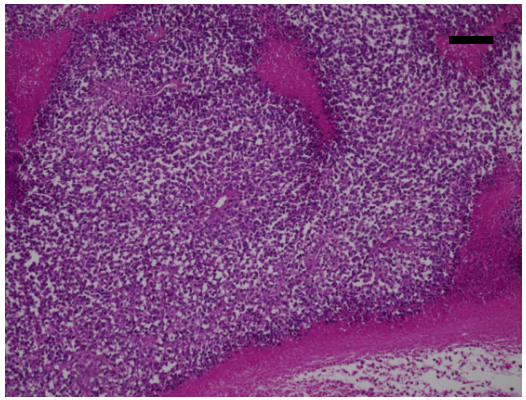

sc HGC27 sphere

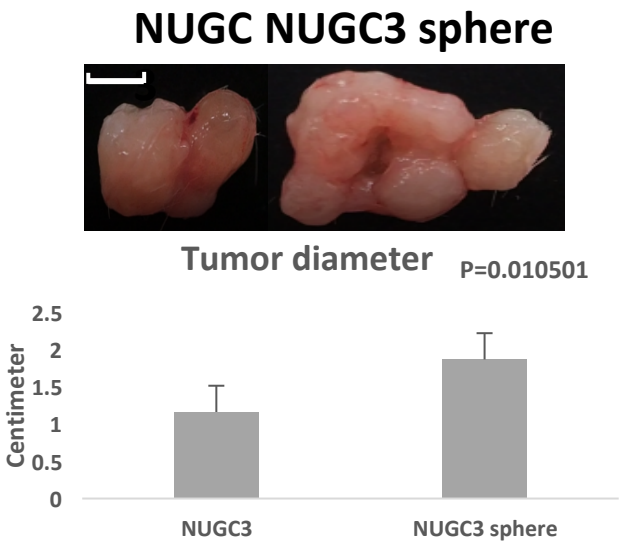

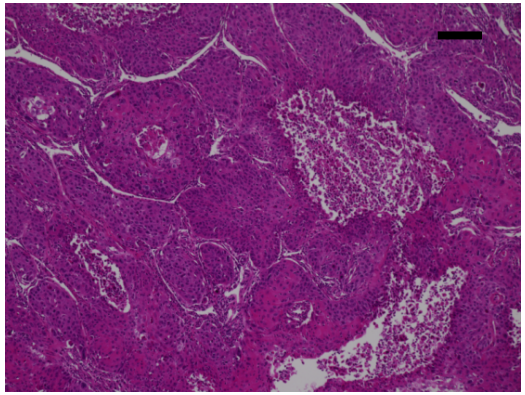

sc NUGC3

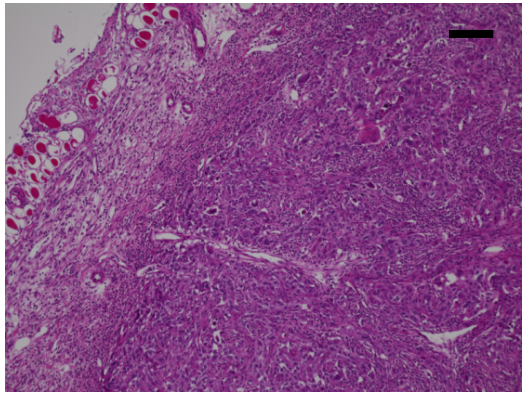

sc NUGC3 sphere

Figure S2